

Tensor Network States: basic introduction

Mari Carmen Bañuls^{1,2}

¹*Max-Planck-Institut für Quantenoptik,*

Hans-Kopfermann-Str. 1, D-85748 Garching, Germany

²*Munich Center for Quantum Science and Technology*

*(MCQST), Schellingstr. 4, D-80799 München**

(Dated: February 8, 2022)

These are some pedagogical notes used to introduce the basic ideas of TNS as (part of) a short course. They are extracted from courses prepared during the last ten years and reflect my personal selection of material, topics and presentation. There are already many comprehensive reviews on the topic at different levels that can be found in the literature (the introduction points to a selection of them).

The notes are in evolution, and this is the version at the date above. The most up-to-date version can be found in [this link](#) (comments or corrections appreciated).

* banulsm@mpq.mpg.de

Contents

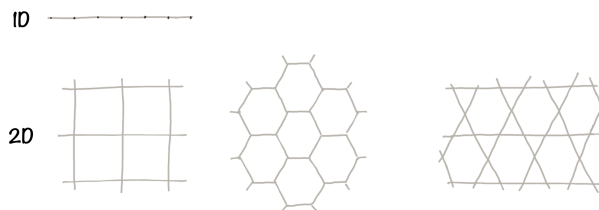
I. Preliminaries	3
A. Introduction	3
B. Graphical notation	6
1. Quantum information concepts	9
II. TNS Ansatzes	12
A. Tensor network states: concepts	12
1. Area law	14
B. Matrix product states (MPS)	15
1. The quantum information construction	15
2. Examples	16
3. Entanglement in MPS	17
4. Canonical form	19
5. Sequential generation	20
6. Expectation values	20
7. Correlations	21
8. MPS and ground states	23
C. PEPS	25
1. Definition	25
2. Examples	27
3. Correlations	29
4. Expectation values and complexity	30
5. Parent Hamiltonians	31
6. Approximation of thermal states	32
7. Boundary theories	33
D. Other families: Tree TN and MERA	35
1. Tree tensor networks (TTN)	35
2. Multiscale entanglement renormalization ansatz (MERA)	39
E. TNS and symmetries	42

III. Representing operators as TN	44
A. Matrix product operators (MPO)	44
1. MPO for local Hamiltonians	44
2. Finite state automata and MPS/MPO	46
3. MPO as ansatz for density operators	48
4. Thermal states	51
B. PEPOs	52
References	52

I. Preliminaries

A. Introduction

We want to study quantum many-body problems on a lattice setting, where the geometry, the lattice spacing and the number of degrees of freedom per site are fixed. Typically we will consider regular lattices (in one or higher dimensions):



This setting may appear, for instance, in magnetism problems (e.g. classical spin models) or in the study of strongly correlated systems. on each site (vertex or edges) of the lattices, there is a finite dimensional degree of freedom (spin, qubit, fermion, ...). The interactions between sites are described by an (effective) Hamiltonian that tries to capture the essential physical features of the system. Some examples are

- the Heisenberg model

$$H = - \sum_{\langle ij \rangle} J_{ij} \vec{S}_i \cdot \vec{S}_j,$$

introduced to describe magnetic ordering in materials;

- the quantum Ising model

$$H = -J \left(\sum_{\langle ij \rangle} S_i^z S_j^z + g \sum_i S_i^z \right),$$

paradigmatic to study quantum phase transitions;

- the Hubbard model

$$H = -t \sum_{\langle ij \rangle} \sum_{\sigma=\uparrow,\downarrow} \left(c_{i\sigma}^\dagger c_{j\sigma} + \text{h.c.} \right) + U \sum_i n_{i\uparrow} n_{i\downarrow},$$

proposed to describe electrons in solids, which describes a transition between conducting and insulating phases, and is a proposed model for high- T_c superconductivity.

In these problems, the goal is to determine

- ground state properties, i.e. phase diagrams, including quantum phase transitions;
- thermal equilibrium properties;
- dynamics, i.e. non-equilibrium behaviour, such as transport properties.

The state of the system can be represented in a tensor product basis. If the k -th site has physical dimension d_k and basis $\{|0\rangle, |1\rangle, \dots, |d_k - 1\rangle\}$ (for instance, $d = 2$ for a qubit or spin 1/2 particle), then the dimension of the whole space is $\mathcal{D} = \prod_{k=1}^L d_k$, and a basis for the whole system can be constructed as

$$\otimes_{k=1 \dots L} \{|0\rangle, |1\rangle, \dots, |d_k - 1\rangle\}.$$

Any state of the global system can be expressed by specifying the \mathcal{D} (exponentially many) coefficients in this basis.

In some cases, these problems can be addressed using analytical techniques. It is the case of exactly solvable models (few) or perturbative regimes (when the main contribution is from an exactly solvable part of the Hamiltonian). But such situations are limited and, in many cases, numerical methods may be the only feasible approach. Specially relevant among such numerical techniques are

- Exact diagonalization (ED) is the most direct method. The ground state, and all energy eigenstates of the system can be found by directly solving the eigenvalue equation for the Hamiltonian $H|\Psi\rangle = E|\Psi\rangle$. There are numerical linear algebra packages that solve this problem. In particular, in the usual case of being interested only in a few eigenvalues at the edge of the spectrum, Lanczos methods can be applied. The cost of the diagonalization scales as \mathcal{D}^3 , i.e. exponentially with the system size. If the problem has symmetries, they can be exploited to reduce the size of the problem by solving it only in the interesting subspace, but ultimately exact diagonalization is limited to systems of a few tens of qubits.
- Quantum Monte Carlo (QMC) methods are a set of computational methods that use Monte Carlo techniques to study different properties (mostly ground state or thermal equilibrium) of large quantum many-body systems. In many circumstances they can provide the most accurate results in polynomial time, but there are particular scenarios where they are hindered by the presence of a so-called *sign problem* (which arises when trying to compute the integral of a highly oscillating function, with positive and negative contributions that require precise estimation to cancel out). This is notably the case for fermionic and highly frustrated systems, where the presence of the sign problem can render the QMC methods exponentially slow.
- Tensor network (TN) methods, which these notes describe, provide an alternative tool to study numerically strongly correlated quantum systems. In particular for one dimensional systems they are nowadays a standard method, actually quasi-exact (see also DMRG¹). The understanding gained from quantum information theory has allowed extensions to higher dimensions and different setups (periodic boundary conditions, time evolution, and more).

An arbitrary state of a quantum many-body system is exponentially expensive to write. Tensor network states (TNS) are entanglement-based ansatzes that try to represent efficiently the physically relevant states of the system.

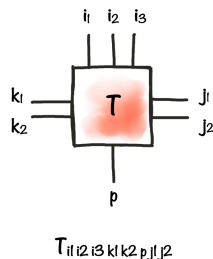
Tensor network methods are successfully used to solve one-dimensional strongly-correlated quantum systems,² but also two-dimensional condensed matter problems³ and quantum chemistry.⁴ They are also applied to study classical statistical problems,^{5,6} and in recent years an increasing effort has been expanding them to other fields (gauge theories, machine learning, ...).

Several introductory and review-like texts about tensor networks can be found in the literature. Some of them could be 7 for a conceptual presentation, 2 and 8 for detailed early reviews about the MPS and PEPS algorithms, or 9–11 for more recent introductory texts, in order of increasing technical details.

B. Graphical notation

The description of TNS properties and algorithms becomes much more simple and intuitive using a pictorial representation.

A tensor is simply a multi-dimensional array, i.e. an object with a number of indices, each of them with a finite (possibly different) dimension. Graphically we represent a tensor with a box, and each of the indices with a leg. For instance, for an 8-rank tensor,



The simplest instances would be a vector v (tensor with one leg) or a matrix M (tensor with two legs),

$$v_i = \text{---} i \text{---} \boxed{v}$$

$$M_{ij} = \text{---} i \text{---} \boxed{M} \text{---} j$$

A particular case is the identity matrix, with elements $\mathbb{1}_{ij} = \delta_{ij}$, which can be represented by a line

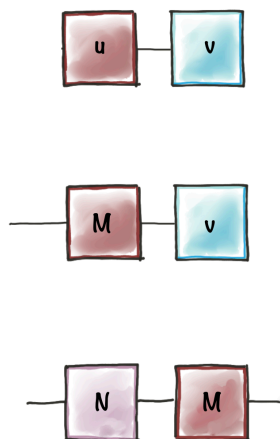
$$\begin{array}{c} i \text{-----} J \\ \hline \end{array} = \delta_{ij}$$

A generalization is the copy tensor, with non-vanishing elements only when all the indices have the same values, which, for the case of rank 3 can be represented as

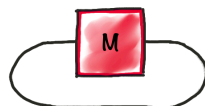
$$\begin{array}{c} \text{-----} J \\ \diagup \quad \diagdown \\ i \text{-----} \quad k \end{array} = \delta_{ijk}$$

Notice that specifying a value for each of the indices, as shown in the figures above, selects a particular component of the tensor, but usually the representation is used to show the whole object (i.e. all components).

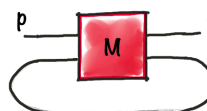
A contraction (product and sum over a shared index) is represented by a leg joining two tensors. For instance for the scalar product of two vectors $\vec{u} \cdot \vec{v}$, for a matrix-vector $\vec{w} = M \cdot \vec{v}$, or a matrix-matrix multiplication $Q = N \cdot M$, we draw



Also the trace of a matrix, or the partial trace in the case of a multidimensional tensor, can be represented in this way



$$= \sum_i M_{ii} = \text{tr } M$$



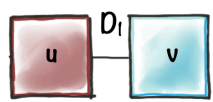
$$= \sum_j M_{pjqj} = \text{tr}_2 M$$

A warning is in order here: there is no unique convention to indicate the transposition or conjugation of a tensor. It can be written explicitly but sometimes it is understood from the context, for instance, if representing the contraction of a vector with itself to compute the norm.

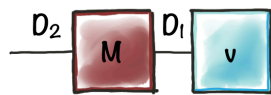
A crucial aspect to consider when talking about algorithms is the computational costs. In TNS algorithms, the leading costs come from the low level tensor manipulations. The running time is estimated by the number of elementary operations needed. For example, the scalar product of two vectors involves a multiplication and a sum for each component, thus has a cost $O(D)$, if the dimension of the vectors is D .

Big-O notation: A function $f(n) = O(g(n))$ if there exist constants $c > 0$ and n_0 such that $\forall n > n_0, |f(n)| \leq c|g(n)|$.

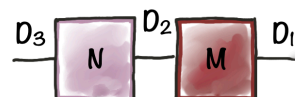
The same is true for each element that needs to be computed in a matrix-vector or matrix-matrix multiplication, which thus have respectively costs $O(D^2)$ and $O(D^3)$ if all the dimensions involved are equal, or, in general



$$O(D_1)$$



$$O(D_1 D_2)$$



$$O(D_1 D_2 D_3)$$

In general, the cost of contracting two tensors (over any number of indices) scales as the product of dimensions of all legs, contracted or not $O(\prod_{j \text{ contracted}} D_j \prod_{k \text{ open}} D_k)$.

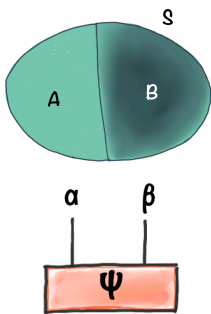
The cost of multiplying two $D \times D$ matrices scales as $O(D^3)$ for the straightforward multiplication. There are more efficient algorithms. The fastest known scales as $O(D^{2.373})$ (but is not practical for matrices of real sizes), and there is a lower bound for the complexity $\Omega(D^2 \log D)$, established by Raz in 2002.

Other operations used often in TNS algorithms are the diagonalization and singular value decomposition. The first one typically is used to find an approximation to the lowest eigenvalue of a matrix, and can be performed via iterative algorithms (based on repeated multiplications) that have a cost $O(D^3)$ for a $D \times D$ matrix. The singular value decomposition for a $m \times n$ matrix has a cost $O(\min(n^2m, nm^2))$.

1. Quantum information concepts

The field of TNS is intimately linked to quantum information theory. Here we just review the indispensable concepts to follow the rest of the lecture. A more complete basic introduction or refresher of quantum mechanical concepts can be found in chapter 2 of.¹²

States of a quantum system are represented as (normalized) vectors in a Hilbert space \mathcal{H} , a complex vector space equipped with an inner product. For a system of physical dimension d , $\mathcal{H} = \mathbb{C}^d$. Using Dirac's notation, vectors are represented as kets $|v\rangle \in \mathcal{H}$, and bras are elements of the dual space $\langle v| \in \mathcal{H}^*$, i.e. linear operators from \mathcal{H} to \mathbb{C} .

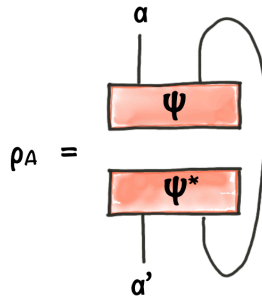


We can consider a composite system, formed by two quantum systems A and B , with Hilbert spaces \mathcal{H}_A and \mathcal{H}_B . The global Hilbert space is the tensor product $\mathcal{H}_S = \mathcal{H}_A \otimes \mathcal{H}_B$. Any pure state can be written as $|\psi_S\rangle = \sum_{\alpha, \beta} \psi_{\alpha\beta} |\alpha\rangle_A \otimes |\beta\rangle_B$, where $\{|i\rangle_{A(B)}\}_{i=0}^{d_{A(B)}-1}$ are orthogonal bases for each subsystem.

The state of one of the subsystems, in general, will be described by the *reduced density matrix* (rdm), for instance, for subsystem A ,

$$\rho_A = \text{tr}_B(|\psi_S\rangle\langle\psi_S|) := \sum_{\beta} \langle\beta_B|\psi_S\rangle\langle\psi_S|\beta_B\rangle = \sum_{\alpha\alpha'} \sum_{\beta} \psi_{\alpha\beta} \psi_{\alpha'\beta}^* |\alpha\rangle\langle\alpha'|.$$

Graphically



This determines the expectation values of any observable that is local to A (i.e. acts only on A) $O_A \otimes \mathbb{1}_B$

$$\langle \psi | O_A | \psi \rangle = \text{tr}(\rho_A O_A).$$

If the state $|\psi_S\rangle$ can be written as a product, $|\psi_S\rangle = |\varphi\rangle_A \otimes |\phi\rangle_B$, we say it is *separable*, and in that case, also the reduced states for A and B are pure (i.e. their reduced density matrices have rank one). Otherwise, the state $|\psi_S\rangle$ is *entangled*. The entanglement entropy is defined as the von Neumann entropy of the reduced density matrix,

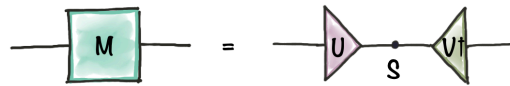
$$S_E = S(\rho_A) := -\text{tr}(\rho_A \log \rho_A).$$

For any density operator ρ , the von Neumann entropy, $S(\rho) = -\text{tr} \rho \log \rho$ has (among others) the following properties

- $S(\rho) \geq 0$;
- $S(\rho) = 0 \Leftrightarrow \rho = |\phi\rangle\langle\phi|$, i.e. iff the state is pure;
- it is maximal, $S_{\max} = \log \mathcal{D}$, for the maximally mixed state $\rho = \mathbb{1}/\mathcal{D}$ (being \mathcal{D} the dimension of the Hilbert space);
- it is invariant under unitary transformations $\rho \rightarrow U\rho U^\dagger$;
- subadditivity: $S(\rho_{AB}) \leq S(\rho_A) + S(\rho_B)$.

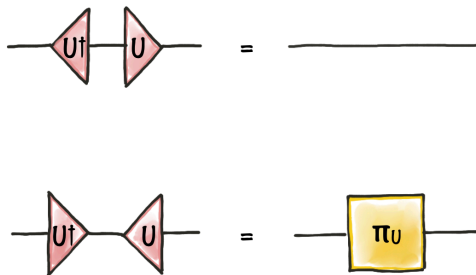
In the case of a pure bipartite state as $|\psi_S\rangle$ above, the entanglement entropy is the genuine measure of entanglement between A and B . For mixed and multipartite systems, on the other hand, quantifying and classifying entanglement becomes much more involved, and is the subject of study of entanglement theory.¹²

An extremely useful concept to characterize entanglement is the Schmidt decomposition, which follows from the singular value decomposition (SVD) of the coefficients matrix $\psi_{\alpha\beta}$ above. Any matrix admits a SVD, of the form $M = USV^\dagger$ (represented graphically in the figure), where S is a diagonal matrix, with real non-negative elements, and U and V are isometries.



For finite dimensional cases, an isometry can be thought of as a part (either a subset of columns or a subset of rows) of a unitary matrix.

In the pictorial representation, isometries are often depicted as triangles and their properties can be represented as



The first line represents the isometric property $U^\dagger U = \mathbb{1}$, and the last line indicates that the result of contracting the isometry with its adjoint over the *small* dimension is a projector. The diagonal elements of S are known as singular values and the rank of the matrix is equal to the number of them which are different from zero. By choosing them to appear in descending order, the SVD factorization of a matrix is unique (up to permutations of degenerate singular values).

By taking the SVD, the coefficient matrix of the state $|\psi_S\rangle$ above can be written as $\psi_{\alpha\beta} = \sum_k U_{\alpha k} \lambda_k V_{k\beta}^\dagger$. The isometries can be used to define two new sets of orthogonal vectors,

$$|u_k\rangle_A = \sum_{\alpha} U_{\alpha k} |\alpha\rangle_A, \quad |v_k\rangle_B = \sum_{\beta} V_{k\beta}^\dagger |\beta\rangle_B,$$

(satisfying $\langle u_k | u_{k'} \rangle = \delta_{kk'}$, $\langle v_k | v_{k'} \rangle = \delta_{kk'}$), in terms of which the state reads

$$|\psi_S\rangle = \sum_k \lambda_k |u_k\rangle_A |v_k\rangle_B.$$

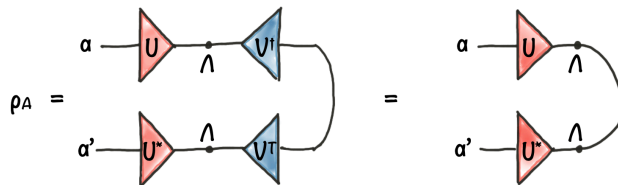
This is known as the *Schmidt decomposition* of the state, and the number of terms in the sum is called *Schmidt rank*. The same as the SVD, the Schmidt decomposition is unique, up to permutations of degenerate Schmidt values.

The Schmidt decomposition of a pure state directly yields the rdm for the subsystems,

$$\rho_A = \text{tr}_B(|\psi\rangle\langle\psi|) = \sum_k \lambda_k^2 |u_k\rangle\langle u_k|, \quad \rho_B = \text{tr}_A(|\psi\rangle\langle\psi|) = \sum_k \lambda_k^2 |v_k\rangle\langle v_k|$$

and thus determines the entanglement entropy $S_E = S(\rho_A) = S(\rho_B) = -\sum_k \lambda_k^2 \log \lambda_k^2$.

Graphically,



If the state of the system is not completely known, we may describe it via a density matrix that represents an ensemble

$$\rho = \sum_i p_i |\varphi_i\rangle\langle\varphi_i|,$$

with $p_i \geq 0$, $\sum_i p_i = 1$. The values p_i represent the probability of having the system in state $|\varphi_i\rangle$ (more generally, we can have $\rho = \sum_i p_i \rho_i$ given as a mixture of mixed states). Notice that the formalism accommodates also the pure case, in which case $\rho = |\psi\rangle\langle\psi|$.

Finally, another useful result from quantum information is the following. For any mixed state of the system ρ_S , we can always find a *purification*, i.e. a pure state of a larger system $|\Psi_{SR}\rangle$ (system S plus ancilla R , where the dimension of the ancilla is at most as large as that of the system) such that $\rho = \text{tr}_R(|\Psi_{SR}\rangle\langle\Psi_{SR}|)$.

II. TNS Ansatzes

A. Tensor network states: concepts

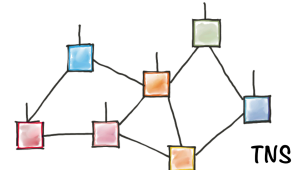
While tensor networks have appeared in different fields, here we are concerned with the description of quantum many-body systems and their physically relevant states. For a system with N individual sites (subsystems), each of them with finite physical dimension d , a general state can be written as



$$|\psi\rangle = \sum_{\{i_1, i_2, \dots, i_N\}=0}^{d-1} C_{i_1, i_2, \dots, i_N} |i_1, i_2, \dots, i_N\rangle,$$

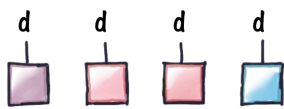
i.e. it is an N -rank tensor, of dimension d^N (graphically in the figure).

In general, tensor network states (TNS) are families of states for which there is a more efficient description. In a TNS the tensor of coefficients has a particular structure, namely that of a tensor network (see illustration). Typically the TNS is constructed out of a polynomial number of small tensors, each of them with a number of components that does not depend on the system size. While any such TNS can be written in the generic form, the converse is not true in general.



The simplest example is that of a product state, such as in a mean field ansatz,

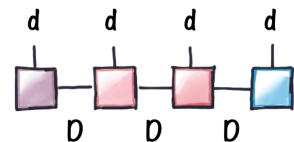
$$\begin{aligned}
 |\psi\rangle &= |\varphi_1\rangle \otimes |\varphi_2\rangle \otimes \dots \otimes |\varphi_N\rangle = \left(\sum_{i_1} c_1^{i_1} |i_1\rangle \right) \otimes \dots \otimes \left(\sum_{i_N} c_N^{i_N} |i_N\rangle \right) \\
 &= \sum_{\{i_1, i_2, \dots, i_N\}=0}^{d-1} c_1^{i_1} c_2^{i_2} \dots c_N^{i_N} |i_1, i_2, \dots, i_N\rangle
 \end{aligned} \tag{1}$$



product state

Each of the coefficients is thus computed as a product of scalar values: one component of each vector. This state can be represented as shown on the left. Because the state is specified by one d -dimensional vector per site, the number of parameters is $O(Nd)$.

To go one step beyond the product ansatz, we may replace the vectors by matrices of a certain dimension $D \times D$. This yields a matrix product state (MPS), which pictorially can be represented as shown on the right. In this case, each C_{i_1, i_2, \dots, i_N} coefficient can be computed as a product of matrices, and the number of parameters scales as $O(NdD^2)$.



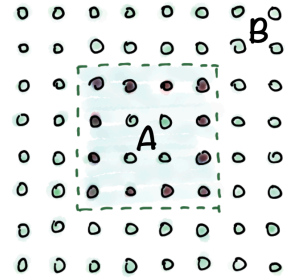
MPS

Notice that TN can also be used to represent other objects, not necessarily pure quantum states. For instance, a TN with no open indices can represent the partition function of a classical model, or the expectation value of particular observables. TN can also be used to write or approximate operators, in particular density matrices.

1. Area law

Having only polynomial number of parameters, a TNS family cannot capture the exponential complexity of the whole Hilbert space. But physical states explore only a small fraction of the latter. And the goal of TNS ansatzes is precisely to describe such region. It turns out that a most remarkable property of equilibrium states is that they contain a very small amount of entanglement.

Let us consider a bipartition of the many-body system into two subsystems A and B (such as illustrated in the figure). For most states in the Hilbert space the entanglement entropy will grow as the number of sites enclosed in (the smallest) subsystem A , i.e. as the *volume* of A (in a regular D -dimensional lattice $S_A \sim L^D$). In contrast, ground states of local Hamiltonians often present a very different behaviour, known as *area law* of entanglement.¹³ A



bipartite state satisfies the area law if the entanglement entropy scales only as the size of the *boundary* between regions A and B ($S_A \sim L^{D-1}$ in a regular lattice as the one depicted in the figure). The area law is rigorously proved in the case of one dimensional gapped local Hamiltonians.¹⁴ For critical systems, which are gapless, the area law is violated, but only with logarithmic corrections, $S_A \lesssim L^{D-1} \log L$, which means that the amount of entanglement in these systems is still much smaller than the generic volume law.

There are also known exceptions¹⁵ for gapless systems for which the gap closes faster than for any critical system described by a CFT and which have not logarithmic but \sqrt{L} corrections to the area law.

Similar behaviour is expected for higher dimensional systems, but there is no mathematical proof for the area law in that case. However, for local Hamiltonians in any dimension, thermal equilibrium states¹⁶ at temperature T strictly satisfy an area law, only for the mutual information, instead of the entanglement entropy. Namely

$$I(A : B) \leq \frac{1}{T} \|h\| |\partial A|,$$

where $\|h\|$ bounds the strength of the interaction and $|\partial A|$ denotes the size of the boundary. Notice that, since the bound in this case scales with the inverse temperature, it does not restrict the ground state ($T = 0$) case.

B. Matrix product states (MPS)

Matrix product states (MPS) are the paradigmatic TNS. As a TNS family, it is the one for which mathematical properties are best understood, and from a practical point of view, they allow for the most efficient algorithms. They are actually at the root of the success of the density matrix renormalization group (DMRG) algorithm,¹ probably the most precise method to study one dimensional strongly correlated quantum systems (and even for some two dimensional problems).

1. The quantum information construction

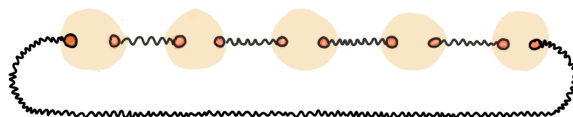
We can introduce the MPS family, as suggested earlier, as a restriction of the general form of the coefficient tensors to a particular structure, where each coefficient is a product of matrices. For a chain of N sites, each of them with physical dimension d ,

$$|\Psi\rangle = \sum_{i_1, \dots, i_N=0}^{d-1} \text{tr} (A_1^{i_1} A_2^{i_2} \dots A_N^{i_N}) |i_1 i_2 \dots i_N\rangle$$

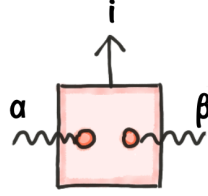
Equivalently, they can be defined from the following construction that makes their entanglement properties immediately apparent. Let us consider a periodic chain of N sites, and assign to each site two virtual systems of dimension D . We choose these systems to be in a state such that the virtual systems that lie at the edges of the same lattice bond are maximally entangled, i.e., they are in a state

$$|\Phi\rangle \propto \sum_{\alpha=0}^{D-1} |\alpha\alpha\rangle$$

Graphically, we can represent the state of the chain as

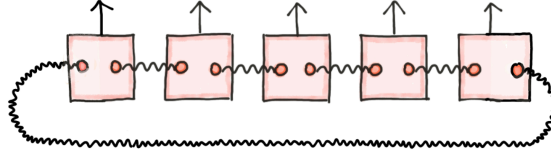


with shaded regions representing the real space sites. The state is thus a product on N such maximally entangled pairs $|\Phi\rangle^{\otimes N}$. In order to obtain a state of the physical degrees of freedom, we introduce, on each site of the chain M , a map P_M that projects the states of both virtual systems residing on the site onto the corresponding physical basis,



$$P_M = \sum_{i, \alpha, \beta} (A_M)_{\alpha\beta}^i |i\rangle \langle \alpha\beta|,$$

where A_M is a rank-3 tensor (with dimension dD^2) that specifies the map, and thus contains the parameters that determine the physical state. In total, these are NdD^2 parameters. After applying these maps to all sites, the state looks like



which is precisely a MPS, since

$$|\Psi\rangle = P_1 \otimes P_2 \otimes \dots \otimes P_N |\Phi\rangle^{\otimes N} = \sum_{i_1, i_2, \dots, i_N=0}^{d-1} \text{tr} (A_1^{i_1} A_2^{i_2} \dots A_N^{i_N}) |i_1 i_2 \dots i_N\rangle.$$

While the construction was explained assuming periodic boundary conditions (PBC), it works also with open boundary conditions (OBC), with the only difference that there would be no maximally entangled pair joining the first and last sites, and the corresponding maps would be rank two tensors of dimension dD .

2. Examples

a. Product state

A product state $|\Psi\rangle = |\varphi_1\rangle \otimes |\varphi_2\rangle \otimes \dots \otimes |\varphi_N\rangle$ is a MPS with $D = 1$. If each individual state (for physical dimension d) is $|\varphi_k\rangle = \sum_{i=0}^{d-1} A_{[k]}^i |i\rangle$, the tensors of the MPS are the $d \times 1 \times 1$ $A_{[k]}$.

b. W-state

The entangled state $|\Psi\rangle = \frac{1}{\sqrt{N}} (|100\dots 0\rangle + |010\dots 0\rangle + \dots + |00\dots 01\rangle)$ for any number of sites N can be written as a MPS with $D = 2$ and tensors (in the middle of the chain)

$$A_{[k]}^0 = \begin{pmatrix} 1 & 0 \\ 0 & 1 \end{pmatrix}, \quad A_{[k]}^1 = \frac{1}{\sqrt{N}} \begin{pmatrix} 0 & 1 \\ 0 & 0 \end{pmatrix}, \quad \text{for } 1 < k < N,$$

and in the edges,

$$A_{[1]}^0 = \begin{pmatrix} 1 & 0 \end{pmatrix}, \quad A_{[1]}^1 = \frac{1}{\sqrt{N}} \begin{pmatrix} 0 & 1 \end{pmatrix},$$

$$A_{[N]}^0 = \begin{pmatrix} 0 \\ 1 \end{pmatrix}, \quad A_{[N]}^1 = \frac{1}{\sqrt{N}} \begin{pmatrix} 1 \\ 0 \end{pmatrix}.$$

c. AKLT ground state

The AKLT model was introduced by Affleck, Kennedy, Lieb and Tasaki¹⁷ as an exactly solvable spin $s = 1$ chain. The construction, which the MPS generalizes is the following. Consider each site has two $s = 1/2$ components (the physical dof is $s = 1$, so their state is projected onto the symmetric subspace), and there is a singlet between each pair of neighboring sites, $\frac{1}{\sqrt{2}}(|00\rangle - |11\rangle)$. Then two neighbouring sites contain four $s = 1/2$ components, but their total spin can never be the maximum (2), since the inner pair is in the singlet configuration. Therefore, projecting two sites onto total spin $S_{(i,i+1)} = 2$ (where $\vec{S}_{(i,i+1)} := \vec{S}_i + \vec{S}_{i+1}$) annihilates such state. If we define the Hamiltonian

$$H_{\text{AKLT}} = \sum_k P(S_{(k,k+1)} = 2) = \sum_k \left[\frac{1}{2} \vec{S}_i \cdot \vec{S}_{i+1} + \frac{1}{6} (\vec{S}_i \cdot \vec{S}_{i+1})^2 + \frac{1}{3} \right],$$

1. it annihilates the state defined before (i.e. the state is an eigenstate with eigenvalue 0);
2. it is positive (as a sum of projectors) and thus the state with eigenvalue 0 is the ground state.

3. Entanglement in MPS

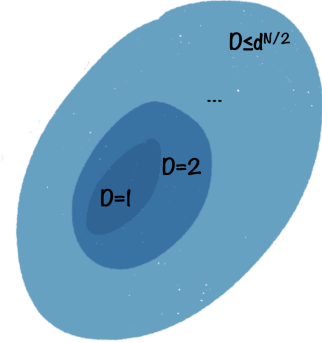
By construction, MPS satisfy the area law. Since the maps P_M are local, they cannot increase the entanglement between sites and all entanglement in the system is already introduced by the state $|\Phi\rangle^{\otimes N}$. If we consider a bipartition of the chain, where subsystem A is taken to be L contiguous sites in the middle, we can thus bound

$$S(\rho_A) \leq S(\text{tr}_{N \setminus A} |\Phi^{\otimes N}\rangle \langle \Phi^{\otimes N}|) = 2 \log D.$$

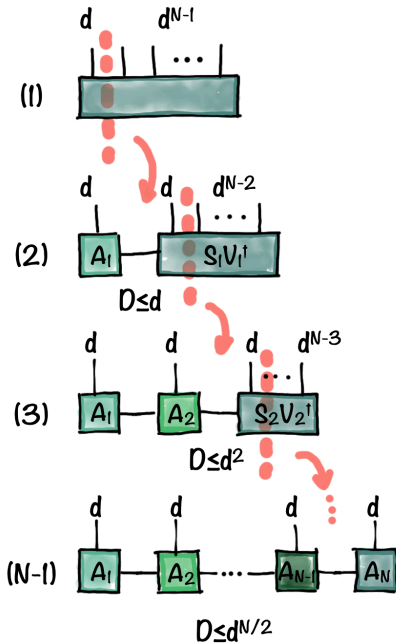
The last equality follows because the maximally entangled pairs that lie completely within region A do not contribute to the entanglement, while both *cut* pairs each contribute $\log D$.

Since in one spatial dimension the size of the boundary of a (connected) region is constant, this corresponds to an area law.

How much a MPS can accommodate is then bounded by the value of the bond dimension D . Moreover, tensors of a certain bond dimension can be embedded in larger ones. The MPS define thus a hierarchy of increasing entanglement as the bond dimension increases, where the set of MPS with fixed D includes all the MPS with smaller bond dimension, as illustrated in the figure. The lowest one $D = 1$ corresponds to product states, and $D = d^{\lfloor N/2 \rfloor}$ is enough to describe exactly the whole Hilbert space.



Indeed, any state can be written as a MPS by sequentially applying SVDs across each bond.



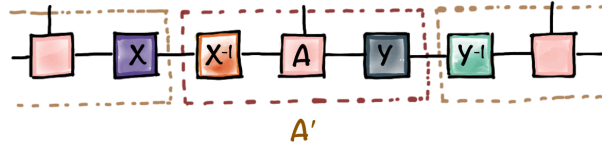
Starting from the left, the coefficient tensor can be reshaped as a $d \times d^{N-1}$ matrix. Applying a SVD can give at most d non-vanishing singular values (the rank being bounded by the smallest dimension of the matrix). Thus we obtain $A_1 \cdot S \cdot V^\dagger$, and identify the left isometry with the first MPS tensor ($d \times D_1$ with $D_1 \leq d$). The product $S_1 \cdot V_1^\dagger$ is a $D_1 \times d^{N-1}$ matrix, on which we apply the same procedure, this time reshaping as $D_1 d \times d^{N-2}$ before performing the SVD. In this case, the maximum number of non-vanishing values will be $D_2 \leq d^2$. By applying successive SVDs to each bond of the chain, we arrive to a MPS form. The bond dimension across each cut is the Schmidt rank of the bipartition across the corresponding bond, with the largest possible value corresponding to the bond closest to the center, so that $D \leq d^{\lfloor N/2 \rfloor}$.

4. Canonical form

We have just concluded that any vector can be written in the MPS form

$$|\Psi\rangle = \sum_{i_1, i_2, \dots = 0}^{d-1} \text{tr} (A_1^{i_1} A_2^{i_2} \dots A_N^{i_N}) |i_1 i_2 \dots i_N\rangle,$$

but the A_k tensors are not unique. We can multiply the virtual indices by any $D \times D$ invertible matrix X , and at the same time multiply the neighbouring tensor by its inverse, such that we redefine the tensors, but the state does not change. Graphically



This is called *gauge freedom*.

In the OBC case it is possible however to choose the gauge such that the MPS tensors satisfy a *canonical form*.¹⁸ This is crucial for formal results, as it allows one to conclude things about states looking only at local properties of the MPS tensors, but plays also a fundamental role in the numerical algorithms, which can be made more efficient by choosing the proper form of the tensors. For the M -th tensor the canonical form reads

$$\begin{aligned} \begin{array}{c} \text{---} \\ | \\ \text{---} \end{array} \begin{array}{c} \text{---} \\ | \\ \text{---} \end{array} \begin{array}{c} \text{---} \\ | \\ \text{---} \end{array} &= \left(\sum_i (A_M^i)^\dagger A_M^i = \mathbb{1} \right) \\ \begin{array}{c} \text{---} \\ | \\ \text{---} \end{array} &= \left(\sum_i A_M^i \Lambda_{M+1} (A_M^i)^\dagger = \Lambda_M \right) \end{aligned}$$

where Λ_M are diagonal positive matrices with full rank. For a normalized state, their diagonal values correspond to the squared Schmidt values for the corresponding cut, i.e. the eigenvalues of the reduced density matrix for the chain up to that point, and $\text{tr} \Lambda_k = 1$. For the first and last sites, $\Lambda_1 = \Lambda_{N+1} = 1$. The canonical form is unique up to permutations of the Schmidt values. Notice that the first part of the canonical condition establishes that, properly reshaped, the MPS tensors are isometries.

This form of writing the canonical form is sometimes called *left canonical*. It is also

possible to choose a *right canonical* form in which the equations are exchanged.

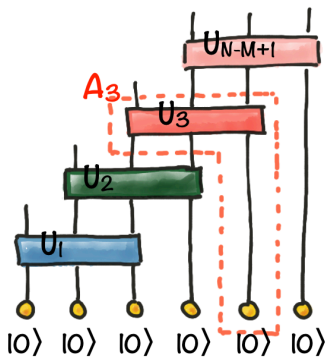
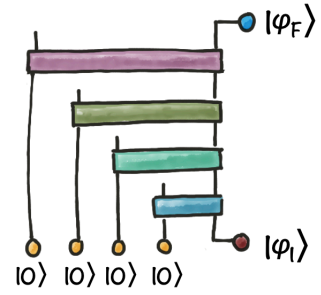
$$\sum_i (A_M^i)^\dagger \Lambda_{M-1} A_M^i = \Lambda_M$$

$$\sum_i A_M^i (A_M^i)^\dagger = \mathbb{1}$$

Given a MPS which is not in canonical form, it is possible to reduce it to it by local matrices. Namely, if $|\Psi\rangle = \sum \text{tr} (B_1^{i_1} \dots B_N^{i_N}) |i_1 \dots i_N\rangle$, then there exist matrices X_k, Y_k with $Y_k X_k = \mathbb{1}_{D_k}$, s.t. $A_k^i = X_{k-1} B_k^i Y_k$ satisfies the canonical form. These matrices can be found with only local operations.

5. Sequential generation

MPS can be equivalently defined as the family of states that can be prepared by sequentially applying a unitary onto an ancillary system of dimension D , initially in a state $|\varphi_I\rangle$, and each of the local systems,¹⁹ initially prepared in a state $|0\rangle$, as sketched in the figure. This means that MPS can be efficiently prepared.



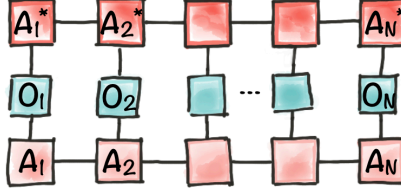
The ancillary system can be replaced by considering unitaries that act on $M = 1 + \log D / \log d$ sites, initially prepared in a state $|0\rangle$. In terms of these unitaries, the MPS tensors (except for the last M) are

$$A_k^i = \langle i\beta | U_k | \alpha 0 \rangle.$$

6. Expectation values

Expectation values of local operators (or tensor products of them) in a MPS can be exactly computed efficiently, i.e. with a cost that scales linearly with the system size. The

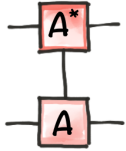
expectation value of an operator of the form $O = O_1 \otimes O_2 \otimes \dots \otimes O_N$ can be represented graphically with the following TN.



For each site k and local operator O_k we can define the following $D^2 \times D^2$ matrix

$$\begin{array}{c}
 \alpha' \text{---} \boxed{A^*} \text{---} \beta' \\
 | \\
 \boxed{O} \\
 | \\
 \alpha \text{---} \boxed{A} \text{---} \beta
 \end{array}
 \quad
 (E_{O_k}^{[k]})_{\tilde{\alpha}\tilde{\beta}} := \sum_{ij} A_{[k]\alpha\beta}^i A_{[k]\alpha'\beta'}^{*j} \langle j|O_k|i\rangle$$

with composite indices $\tilde{\alpha} := (\alpha\alpha')$, $\tilde{\beta} := (\beta\beta')$. For the particular case of the identity operator $O_k = \mathbb{1}$, this is the *transfer matrix*



$$E^{[k]} := \sum_i A_{[k]}^i \otimes A_{[k]}^{*i}$$

Notice that this object is central in the gauge conditions, and the canonical form can also be read as properties of the transfer operator.

The expectation value of the tensor product above can then be written as a product of $D^2 \times D^2$ matrices (for OBC the first and last ones will just be vectors $1 \times D^2$ and $D^2 \times 1$).

$$\langle \Psi|O|\Psi \rangle = E_{O_1}^{[1]} E_{O_2}^{[2]} \dots E_{O_N}^{[N]}$$

which can be computed with cost $O(ND^4)$. In the PBC case, the expectation value reduces to a trace of a product of matrices, and the cost will be bounded as $O(ND^6)$.

Using the TN structure of the transfer operators, the cost in the OBC case can be reduced to $O(ND^3)$, and to $O(ND^5)$ in the PBC case.

7. Correlations

In a MPS, two-point correlations decay exponentially. Let us define the connected two-point correlator

$$C_{O_1 O_2}(x, x + \ell) := \langle O_1^{[x]} O_2^{[x+\ell]} \rangle - \langle O_1^{[x]} \rangle \langle O_2^{[x+\ell]} \rangle,$$

and consider a translationally invariant case (i. e. all tensors are equal $A_k =: A$), for a chain in the thermodynamic limit $N \rightarrow \infty$ (in which case the boundary conditions are irrelevant). In such case, the correlator depends only on the distance ℓ , and not on the position x . In terms of the transfer operators introduced before, the expectation value of a single-site operator O_i ($i = 1, 2$) can be written

$$\langle O_i \rangle = \lim_{N \rightarrow \infty} \frac{\text{tr}(E^{N-1} E_{O_i})}{\text{tr}(E^N)}.$$

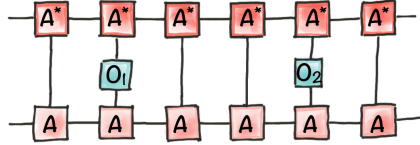
Let the spectral decomposition of the transfer matrix be

$$E = \sum_p \mu_p |R_p\rangle \langle L_p|,$$

where $|R_p\rangle$ and $\langle L_p|$ are the right and left eigenvectors of the transfer matrix, and μ_p the corresponding eigenvalues in order of decreasing absolute value. In the generic case, which we consider here, there is a unique eigenvalue with the largest absolute value $\mu_1 = 1$, and the rest $|\mu_p| < 1$ for $p > 1$. Thus,

$$\frac{\text{tr}(E^{N-1} E_{O_i})}{\text{tr}(E^N)} \xrightarrow{N \rightarrow \infty} \frac{1}{\mu_1} \langle L_1 | E_{O_i} | R_1 \rangle,$$

and for the two-body operator, which corresponds to the following TN



$$\langle O_1^{[0]} O_2^{[\ell]} \rangle = \lim_{N \rightarrow \infty} \frac{\text{tr}(E^{N-\ell-1} E_{O_1} E^{\ell-1} E_{O_2})}{\text{tr}(E^N)} = \frac{1}{\mu_1^{\ell+1}} \langle L_1 | E_{O_1} \left[\sum_p \mu_p^{\ell-1} |R_p\rangle \langle L_p| \right] E_{O_2} | R_1 \rangle.$$

The first term in the sum, $p = 1$, is precisely the disconnected contribution $\langle O_1 \rangle \langle O_2 \rangle$, such that the leading contribution to the connected correlator is

$$C_{O_1 O_2} = \frac{1}{\mu^2} \left[\left(\frac{\mu_2}{\mu_1} \right)^{\ell-1} \langle L_1 | E_{O_1} | R_2 \rangle \langle L_2 | E_{O_2} | R_1 \rangle + \dots \right].$$

Since $|\mu_2| < |\mu_1|$, the correlation decays exponentially with the distance ($e^{-\ell/\xi}$) with correlation length $\frac{1}{\xi} = -\log \left| \frac{\mu_2}{\mu_1} \right|$.

Although MPS cannot hold critical (i.e. algebraically decaying) correlations, in practice it can still be used to study critical systems: it approximates the correlations for larger distances as D is increased, and there is *entanglement scaling*.²⁰

The non generic case is that of non-injective MPS, which can accommodate non-decaying correlations (example: the GHZ state).

8. MPS and ground states

MPS approximate ground states of local Hamiltonians efficiently.^{14,21}

a. Truncation error

While a generic state can be exactly written as a MPS, this may require an exponentially large bond dimension, up to $d^{\lfloor N/2 \rfloor}$. We can construct a MPS approximation with bounded bond dimension D by *truncating* the Schmidt values for each bond and keeping only the largest D . The resulting error can be bounded as

$$\| |\Psi\rangle - |\Psi_D\rangle \|^2 \leq 2 \sum_{\alpha=1}^{N-1} \varepsilon_{\alpha}(D),$$

where the sum runs over the bonds and for each of them, if the exact bond dimension is D_{α} , $\varepsilon_{\alpha}(D) := \sum_{i=D+1}^{D_{\alpha}} |\lambda_{[\alpha]_i}|^2$.

As a corollary of this result, the error in the MPS approximation of a given state depends on how fast the Schmidt coefficients decay. In particular, for ground states of local gapped Hamiltonians,¹⁴ said coefficients satisfy (for each cut)

$$\sum_{k>D} |\lambda_k|^2 \leq C D^{-1/(6\xi \log d)},$$

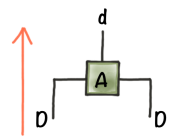
where C is a constant, and ξ a correlation length (more precisely $\xi = \max(\frac{v}{\Delta E}, \xi_c)$, with ΔE the energy gap, and v and ξ_c the velocity and length scale in the Lieb-Robinson bound,²² which control the propagation of correlations).

The error from cutting the Schmidt values can be related to the Rényi entropy which, in case of critical systems in 1D, scales, for a block of size L , as $\log(L)$. As a consequence, ground states of critical 1D Hamiltonians for a finite size, can be approximated with fixed error by a MPS with bond dimension that grows polynomially in the system size.²¹

b. Parent Hamiltonians

Every MPS is the ground state of a local Hamiltonian. If the MPS is injective, the ground state is unique.

A MPS tensor A is called *injective* if the map it defines from virtual to physical degrees of freedom,

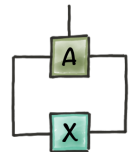


$$\mathcal{P}(A) : \mathbb{C}^{D \times D} \rightarrow \mathbb{C}^d$$

$$\mathcal{P}(A) := \sum_{i, \alpha, \beta} A_{\alpha\beta}^i |i\rangle \langle \alpha\beta|,$$

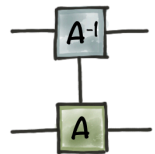
(2)

is injective. \mathcal{P} maps a $D \times D$ matrix X to a vector $v(X)$ in the local physical space,

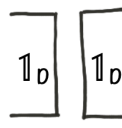


$$v(X) = \sum_i \text{tr}(A^i X^T) |i\rangle.$$

The injectivity property means that no two matrices of the domain are mapped to the same vector (equivalently, the kernel is only the null vector), and it is equivalent to the existence of a *left inverse* of the A tensor,



=



If the tensor is injective, by acting on the physical index we can access all the virtual (boundary) space. Injectivity is a generic condition: we can coarse-grain the chain, blocking sites together and defining larger physical spaces. The physical dimension scales then as d^ℓ for a block of size ℓ , while the virtual dimension does not change, and thus the dimension of the physical leg becomes much larger. It is also equivalent to the tensor having a single block in the canonical form.

$$A^i = \begin{pmatrix} A_{(1)}^i & & \\ & A_{(2)}^i & \\ & & \dots \end{pmatrix}$$

In the non-injective case, the canonical form is block diagonal, with each diagonal block satisfying the canonical form conditions. This structure cannot span the whole space of $D \times D$ matrices. Moreover, correlations may have a long-range non-decaying part.

Any injective MPS (i.e. all the tensors are injective) is the unique ground state of a local *frustration-free* Hamiltonian. We can construct explicitly the *parent Hamiltonian* for any MPS $\Psi = \sum \text{tr}(A_1^{i_1} A_2^{i_2} \dots A_N^{i_N}) |i_1 i_2 \dots i_N\rangle$ (injective or not). We define the subspace \mathcal{S}_2 spanned by each pair of tensors²³

$$\mathcal{S}_2^{[k]} := \left\{ \begin{array}{c} \text{Diagram: A circuit with two parallel paths. The top path contains two green boxes labeled 'A' connected by a horizontal line. The bottom path contains a single green box labeled 'X'. The two paths are connected by vertical lines at both ends, forming a closed loop.} \\ ; X \in \mathbb{C}^{D \times D} \end{array} \right\}$$

and denote by $\Pi_{\mathcal{S}_2^{[k]}}$ the corresponding projector. The parent Hamiltonian can be defined as the sum of the orthogonal projectors,

$$H_{\text{parent}} := \sum_k \left(\mathbb{1} - \Pi_{\mathcal{S}_2^{[k]}} \right).$$

Being a sum of projectors, $H_{\text{parent}} \geq 0$, and since it annihilates the MPS, $H_{\text{parent}}|\Psi\rangle = 0$, then $|\Psi\rangle$ is a ground state. If the MPS is injective, it can be shown that the ground state is unique.

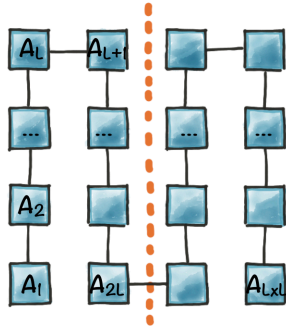
MPS can be identified as the suitable class of states to describe ground states of local Hamiltonians.

The parent Hamiltonian construction also applies to PEPS for the two dimensional case. It can be shown that injective PEPS are also unique ground states of local frustration free Hamiltonians. But the implication does not work in the opposite direction.

C. PEPS

Projected entangled pair states (PEPS) are the natural generalization of the MPS construction to higher dimensions.

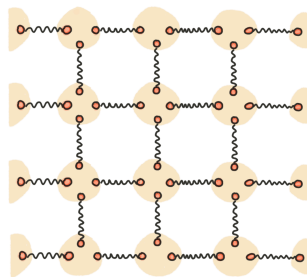
1. Definition



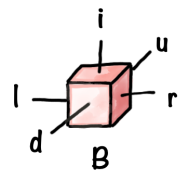
Since MPS are a universal family, it is possible to write also the state of a two dimensional system as a MPS. One needs to select a linear order for the sites in the system, for which different options exist. One of them is the so-called *snake* (shown in the figure). But we can split the system in two by cutting only one bond (as shown), and because the entanglement with respect to this partition is upper bounded by $\log D$, in order to describe a state which satisfies the entanglement area law, the bond dimension will need to scale as D^L (for a $L \times L$ system). While the snake-MPS is used in practice to study two dimensional systems, due to this reason they have to be chosen to be narrow in one direction. Also notice that once the linear ordering of sites is selected, interactions that are local in the original lattice get mapped to long range ones.

Although other orderings of the sites are possible, and some can reduce the range of non-local interactions and improve the efficiency, but they can not produce an area law.

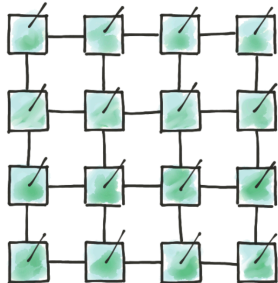
The quantum information construction of MPS starting from pairs of maximally entangled virtual particles can be naturally generalized to any lattice geometry by placing one such pair along each bond in the lattice. In particular, for a regular two dimensional lattice this inserts four virtual particles per site (except at the edges of the lattice),



Then the virtual degrees of freedom residing in each lattice site are mapped onto the physical degrees of freedom by a map $\mathcal{P} = \sum_{i,\ell,r,u,d} B_{\ell r u d}^i |i\rangle \langle \ell r u d|$. This corresponds to a rank-5 tensor, graphically represented on the right.



The PEPS ansatz results from contracting all the tensors over the edges, which we can represent as



$$|\Psi\rangle = \sum_{i_1 \dots i_N} c\left(\{B_{[k]}^{i_k}\}\right) |i_1 \dots i_N\rangle.$$

Notice that the same construction applies to higher dimensions, and also to any lattice geometry, resulting in tensors of different rank.

By construction, PEPS automatically satisfy an area law. The argument is the same as for the MPS construction, since the entropy of a region is upper bounded by that of the maximally entangled pairs before applying the local maps. In this case, for a region A with boundary of size $|\partial A|$, the bound is $S_A \leq \log D^{|\partial A|}$.

Since they include MPS (the snake construction above is obviously a PEPS where some of the bonds have dimension 1), PEPS are also a complete family, capable of describing the whole Hilbert space if the bond dimension is large enough (up to $d^{\lfloor L^2/2 \rfloor}$ for a $L \times L$ square lattice).

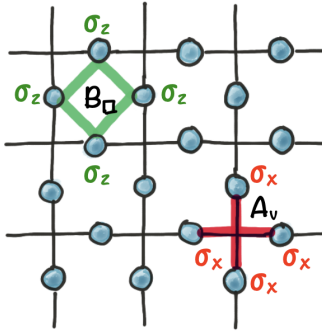
2. Examples

a. MPS

PEPS include the MPS family, which constitute an efficiently contractible subset of PEPS (one which, according to the argument above, cannot contain enough entanglement to reproduce the area law). For instance, looking at the snake-MPS shown earlier, we can reinterpret each tensor as a 4-legged one, with bond dimension one in the directions perpendicular to the snake.

b. Toric code

A much less trivial example is that of the ground state of the toric code Hamiltonian. The toric code was introduced by Kitaev²⁴ as the first instance of topological quantum computation. The model is defined on a square lattice, with the spin $s = 1/2$ degrees of freedom residing on the links. The Hamiltonian reads



$$H = -J_A \sum_v A_v - J_B \sum_{\square} B_{\square},$$

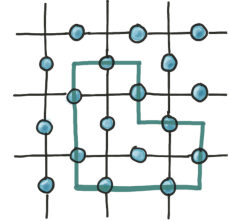
with $J_{A(B)} > 0$, and where the first sum runs over each vertex v of the lattice, and the second one over all the plaquettes. The corresponding operators are 4-body interactions reading $A_v = \sigma_{v_1}^x \sigma_{v_2}^x \sigma_{v_3}^x \sigma_{v_4}^x$ and $B_{\square} = \sigma_{p_1}^z \sigma_{p_2}^z \sigma_{p_3}^z \sigma_{p_4}^z$, with products of operators acting respectively around a vertex or a plaquette (as illustrated in the picture).

All A and B terms commute with each other, and thus the ground state is an eigenstate of all of them (i.e. frustration free), satisfying

$$A_v |\Psi\rangle = B_{\square} |\Psi\rangle = |\Psi\rangle, \quad \forall v, \square.$$

The B_{\square} restrictions means an even number of $|1\rangle$ around each plaquette, which requires closed loops, while the A_v term moves such loops and thus favours an equal superposition of all possibilities.

The ground state in an infinite lattice is unique and corresponds to an equal superposition of loop configurations (or *quantum loop gas*) as the one illustrated in the figure, where the sites traversed by the loop are in state $|1\rangle$ and the rest in $|0\rangle$. This can also be written (up to normalization) as



$$|\Psi\rangle \propto \prod_v (\mathbb{1} + A_v) |0\rangle^{\otimes N}.$$

$$\mathbb{1} + \sigma_x \otimes \sigma_x \otimes \sigma_x \otimes \sigma_x$$

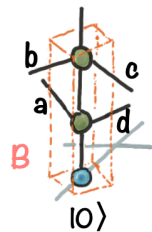


Each of the $(\mathbb{1} + A_v)$ terms can be exactly expressed as a (periodic) MPO of bond dimension 2, acting on the four sites around a vertex, with tensors

$$M_1 = \begin{pmatrix} \mathbb{1} & 0 \\ 0 & \sigma^x \end{pmatrix}.$$

By taking the product of all such operators, and grouping together the ones acting on the same site (two of them), and applying them to $|0\rangle$ we can write the explicit tensors of the PEPS as

$$B_{abcd}^0 = \delta_{ad} \delta_{bc} \delta_{ab}, \quad B_{abcd}^1 = \delta_{ad} \delta_{bc} (1 - \delta_{ab}).$$



Notice that in one half of the sites the tensor (i.e. the identification of indices a, b, c, d) is rotated with respect to the other half.

3. Correlations

In contrast to MPS, PEPS can hold correlations that decay as a power law, even with very small bond dimension. This is so because one can construct quantum states that encode the partition function of a classical spin model, in such a way that the correlations in the state exactly reproduce those of the classical model, also at criticality. In particular, for the 2D classical Ising model, the Hamiltonian reads $H(\{s\}) = -\sum_{\langle ij \rangle} s_i s_j$ for classical spin variables $s_i \in \{-1, +1\}$, and the partition function at inverse temperature $\beta = 1/T$ is $Z_\beta = \sum_{\{s\}} e^{-\beta H(\{s\})}$, with the sum running over all possible configurations of the spins.

for a lattice with a total number of sites N , we can define a quantum state

$$|\Psi_{H,\beta}\rangle := \frac{1}{\sqrt{Z_\beta}} \sum_{\{s_i\}} e^{-\frac{\beta}{2} H(s_1, s_2, \dots, s_N)} |s_1 s_2 \dots s_N\rangle,$$

where the local basis states $|s_k\rangle = |\pm 1\rangle$ can be taken to be the eigenstates of σ_z^k . The expectation values in the z basis can be readily computed, for instance for σ_z on site k ,

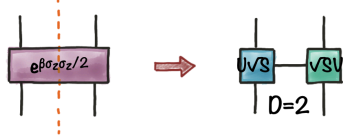
$$\langle \Psi_{H,\beta} | \sigma_z^{[k]} | \Psi_{H,\beta} \rangle = \frac{1}{Z_\beta} \sum_{\{s\}} s_k e^{-\beta H(\{s\})},$$

i.e. they equal the corresponding value of the classical model. The same is true for two-point correlations. The latter has a critical temperature at $\beta = \frac{\log(1+\sqrt{2})}{2}$ at which correlations decay as a power law, $\langle s_0 s_r \rangle \sim \frac{1}{\sqrt{r}}$ for two sites at distance r .

The state $|\Psi_{H,\beta}\rangle$ can be written exactly as a PEPS with bond dimension $D = 2$, for any value of β (in particular for the critical one). We notice that, because σ_z is diagonal in this basis,

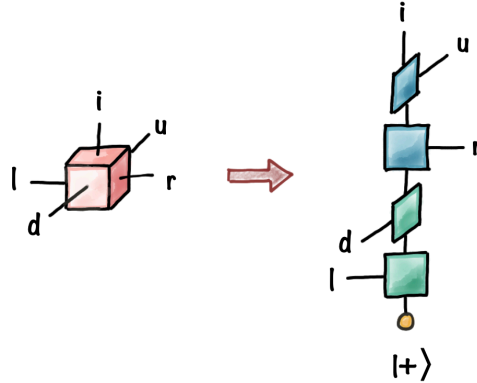
$$|\Psi_{H,\beta}\rangle := \frac{1}{\sqrt{Z_\beta}} \prod_{\{s_i\}} e^{\frac{\beta}{2} \sigma_z^{[i]} \sigma_z^{[j]}} \sum_{\{s_i\}} |s_1 s_2 \dots s_N\rangle.$$

Thus the state is the result of applying a number of two-body operations of the form $e^{\frac{\beta}{2} \sigma_z^{[i]} \sigma_z^{[j]}}$ on each of the edges of the lattice, on an initial state $\sum_{\{s_i\}} |s_1 s_2 \dots s_N\rangle = (|0\rangle + |1\rangle)^{\otimes N} / 2^{N/2}$, which is a product state. By simply writing the Taylor series for the exponentials, we can express each of the two-body operators as a sum of two product terms (equivalently, we could apply a SVD to the operator)



$$e^{\beta\sigma_z^{[i]}\sigma_z^{[j]}/2} = \cosh \frac{\beta}{2} \mathbb{1} \otimes \mathbb{1} + \sinh \frac{\beta}{2} \sigma_z^{[i]} \otimes \sigma_z^{[j]}.$$

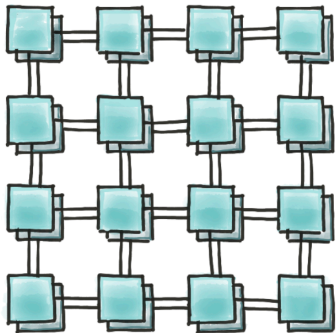
By grouping together all operators acting on the same site, we obtain an explicit form of the PEPS tensors, with bond dimension $D = 2$, which we can represent as



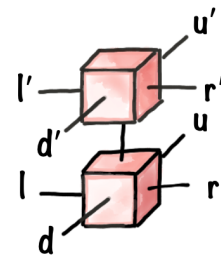
While this shows that PEPS can hold critical correlations with a small bond dimension, it does not mean that any critical state can be written as a PEPS. States as the one presented here are special because they represent classical critical states. For quantum critical states (ground states of a quantum model at a critical point) evidence suggests that an infinite bond dimension may be needed.^{25,26}

4. Expectation values and complexity

Different to MPS, contracting a PEPS, for instance to compute its norm, cannot be done efficiently. The TN representing the norm is shown in the figure,

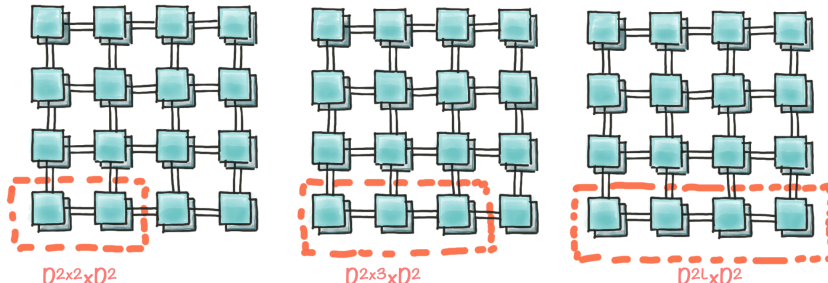


with every local tensor being a *double layer* object, where the PEPS tensor and its conjugate are contracted over the physical index.



While in the one-dimensional analogous picture, this is a product of matrices with constant dimension, the situation is very different now. If we start contracting together the tensors

for a region of the lattice, we always get an object of increasing dimensions as we keep adding tensors, such that the cost of the exact contraction grows exponentially with the system size, as seen explicitly for instance in the sequence below



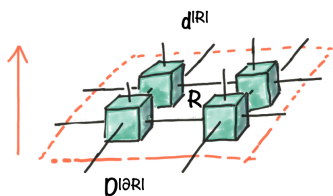
In fact, it is known²⁷ that the problem of contracting an arbitrary PEPS is $\#P$ (the complexity class of counting satisfying assignments of a Boolean formula).

Preparing the state is also a task that cannot be done efficiently for an arbitrary PEPS, different to the sequential scheme of MPS. Creating an arbitrary PEPS has been shown to be in the PP complexity class (determining whether the number of satisfying assignments in the Boolean formula is more than half), which is harder than NP , BQP and QMA . However, one can define subfamilies of PEPS which inherit the property of being efficiently preparable and contractible. as the *sequentially generated states*.²⁸

Even though an exact contraction is not possible, there are approximate contraction schemes that allow practical calculations, at the cost of introducing an additional truncation.

5. Parent Hamiltonians

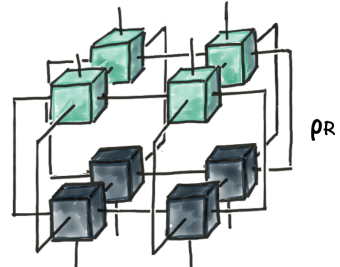
The parent Hamiltonian construction for MPS generalizes for the PEPS case: every PEPS is the ground state of a local, frustration free Hamiltonian and, if the PEPS is injective, the ground state is unique.^{23,29} The basic argument is the following.



If we consider a region R of the lattice, the corresponding block of tensors, as shown in the figure, maps the virtual dimensions on the boundary of the region, dimension $D^{|\partial R|}$ onto the physical degrees of freedom of the block $d^{|R|}$.

The size of the boundary grows much slower than the number of sites in the region so that, as in the MPS case, injectivity of the *boundary-to-physical* map is the generic property. A PEPS is said to be injective if it can be split in disjoint injective regions.

A parent Hamiltonian can be easily constructed noticing that the rank of the $(d^{|R|} \times d^{|R|})$ reduced density matrix for the region R (shown on the right) is upper-bounded by $D^{|\partial R|}$, so that for big enough R it will have a non-trivial kernel.



Now we can construct a local Hamiltonian h acting on R that fulfills $h \geq 0$ and whose kernel coincides with the support S_R or ρ_R . This can be extended to the whole lattice tensoring the operator h with identity, and thus

$$H = \sum_v h_v \times \mathbb{1}$$

(where v runs over all regions and the identity, for each term, acts on the complement of R_v) has the PEPS as ground state, since $\langle \Psi | H | \Psi \rangle = \sum_v \text{tr}(\rho_v h_v) = 0$. Notice that this step does not require injectivity of the region R (only that the support of ρ_R is not the whole Hilbert space, in which case the Hamiltonian would be the null operator). To make the ground state unique, we need to consider two neighbouring injective regions together and construct a local Hamiltonian acting on both, in a generalization of the AKLT construction.

In the PEPS case, different than for MPS, injectivity is not a necessary condition for the uniqueness of the ground state of the parent Hamiltonian:²⁹ there are non-injective PEPS for which such uniqueness can be proved.

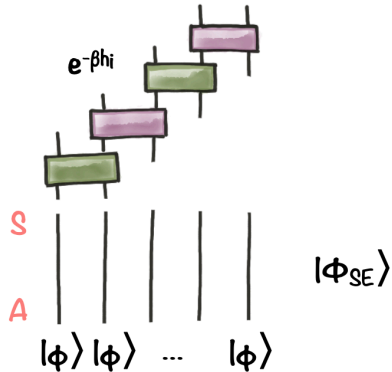
6. Approximation of thermal states

PEPS can approximate thermal equilibrium states of local Hamiltonians in any dimension^{30,31} with polynomial D . In particular, for error ε , $D = \left(\frac{N}{\varepsilon}\right)^{O(\beta d \log_2 d)}$.

The starting idea of the proofs is to construct a purification for the thermal state $\rho_\beta \propto e^{-\beta H}$ of the form (up to normalization)

$$|\Psi\rangle = \left(e^{-\beta H}\right)_S \otimes \mathbb{1}_E |\Phi_{SE}\rangle,$$

where the subindices S and E refer to the system and the ancilla (environment), i.e. $\text{tr}_E |\Psi\rangle\langle\Psi| = \rho_\beta$.



The state $|\Phi_{SE}\rangle = |\phi\rangle^{\otimes N}$ is the product of a maximally entangled state $|\phi\rangle \propto \sum_\alpha |\alpha\alpha\rangle$ of each system site with an ancillary site, and the exponential operator acts on the system side. In the case of mutually commuting terms in the Hamiltonian, the exponential can be broken down to a product of two body terms (as illustrated in the figure), and using their SVD, the result is then directly a *projected entangled pair operator* or PEPO.

In the general case, the terms in the Hamiltonian do not commute with each other. Then the exponential can be written as a Trotter (or alternative) expansion, followed by a compression of the result to a PEPS.

7. Boundary theories

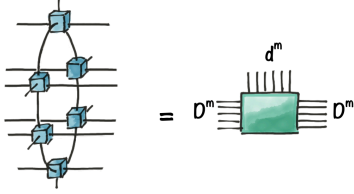
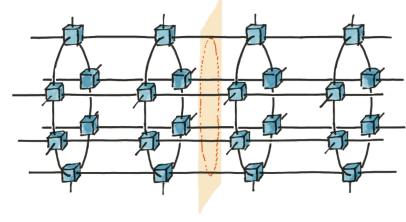
PEPS realize a holographic bulk-boundary relation.

The holographic principle states that the information of a region (physical dof) depends only on its boundary (virtual bonds limiting the region). Conjectured first in the context of black holes, where the entropy is determined by the area, it has a most prominent realization in the AdS/SFT correspondence. But other setups manifest this holographic property, too

- the area law of ground and thermal equilibrium states;
- the entanglement spectrum for a region of certain two-dimensional ground states is found to resemble the low energy sector of a critical one-dimensional model. For a given region, the entanglement spectrum is minus the logarithm of the eigenvalues of the corresponding reduced density matrix.

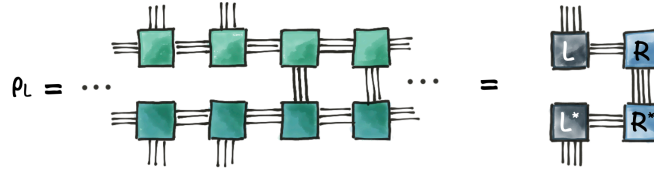
PEPS realize precisely this type of correspondence in a natural manner: the reduced density matrix of a bulk region in a 2D PEPS is supported on the one-dimensional virtual boundary, and the degrees of freedom on which the *entanglement Hamiltonian* acts are precisely the virtual ones on the boundary of the region.^{32,33}

For concreteness, we consider a PEPS on a cylinder of circumference m , and a cut, perpendicular to the cylinder, that divides the system in two, as illustrated in the figure.



To simplify the diagrams, we represent each column of the cylinder as a single tensor (see picture on the left), and then the reduced density matrix of the left part, obtained by tracing out the physical indices of the columns to the right of the cut, can be represented by a one-dimensional diagram.

Furthermore, if we group all the contracted (respectively open) physical indices in a single tensor,



Now we can make use of the polar decomposition of each of the “half-chain” tensors,

$$\begin{aligned}
 L &= U_L J, & \text{with } J &= \sqrt{L^\dagger L} =: \sqrt{\sigma_L} \\
 R &= K V_R, & \text{with } K &= \sqrt{R R^\dagger} =: \sqrt{\sigma_R},
 \end{aligned}$$

where U_L and V_R are unitary matrices, and J, K are positive. Substituting this in the rdm, we can finally write

$$\rho_L = U_L \sqrt{\sigma_L} \sigma_R \sqrt{\sigma_L}^T U_L^\dagger.$$

In this expression, U_L simply represents a map between the support of the rdm and the physical indices, i.e. a bulk region. Since it is an isometry, it does not change the spectrum. This is determined by the matrix $\sqrt{\sigma_L}\sigma_R\sqrt{\sigma_L^T}$, which acts on the virtual degrees of freedom of the boundary. Then a *boundary Hamiltonian* can be constructed as

$$H_b := \log \left(\sqrt{\sigma_L}\sigma_R\sqrt{\sigma_L^T} \right),$$

defined on the boundary degrees of freedom.

The *locality* of the entanglement Hamiltonian is related to the contractibility of the PEPS: if the Hamiltonian is local, then the product of σ matrices can be approximated by a MPO with bond dimension that scales polynomially with m (number of bonds in the boundary). This means that the PEPS can be contracted efficiently (since the contraction of half the system can be approximated by a MPO). Moreover, using PEPS that represent exact ground states in different phases, it has been observed that for a gapped phase with local order, the boundary Hamiltonian is local, while the interaction length diverges when approaching a critical point (see³²).

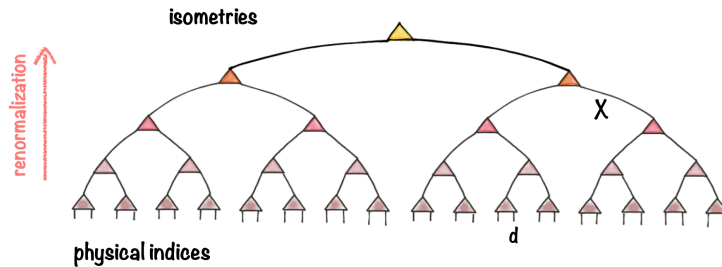
From the mathematical point of view, PEPS are much more complex than MPS, and many fundamental questions remain open.³⁴ Some of them are linked to undecidability results.³⁵ A complete recent review of the mathematical aspects of MPS and PEPS can be found in.³⁶

D. Other families: Tree TN and MERA

1. Tree tensor networks (TTN)

While MPS are extremely useful for numerical studies of even critical systems (thanks to tools as finite size and finite entanglement scaling), they do not reproduce the scaling of correlations characteristic of critical points. This motivated the invention of other families of tensor networks that capture a larger amount of entanglement. The first example is that of tree tensor networks (TTN),³⁷ in which the coefficients of the state are restricted to a TN

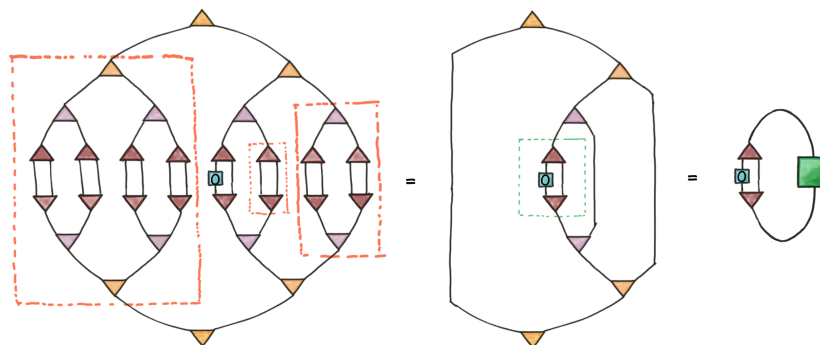
with a tree structure. For instance, for a binary tree, with maximal bond dimension χ , the TN looks like



All the tensors in the tree can be chosen to be isometries, which implies that the state is normalized.

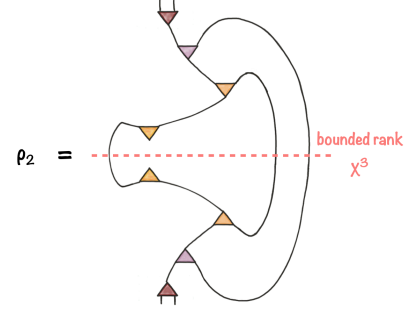
Different to the MPS and PEPS ansatzes discussed until now, the TTN has an additional *renormalization* dimension (vertical in the figure). The tree indeed implements a real space renormalization by reducing the physical degrees of freedom to virtual ones, such that the system is successively coarse-grained, and higher layers represent larger scales. In going up, i.e. passing from a smaller to a larger scale, short-range information is discarded (by the isometries).

Local observables can also be computed efficiently. For instance, for a one-site operator, and making use of the isometric property of the tensors,

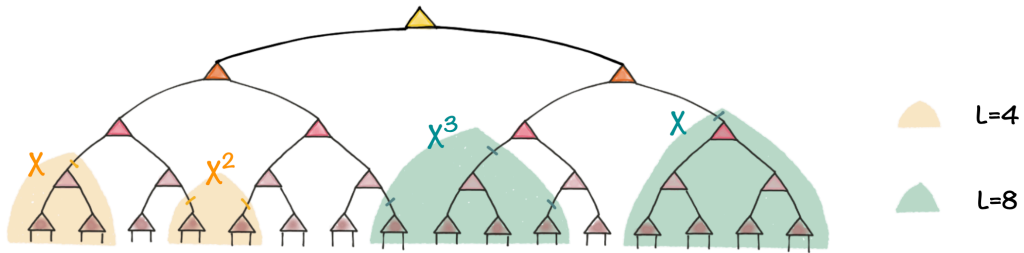


where the last step is simply the result of contracting together everything outside the green dashed box.

Actually, looking at the middle picture from inside out, we can read the rdm for two sites, as the figure explicitly shows. From this construction, we can see that the rank of the rdm is bounded by the product of the dimensions of the virtual legs that cross the red line.

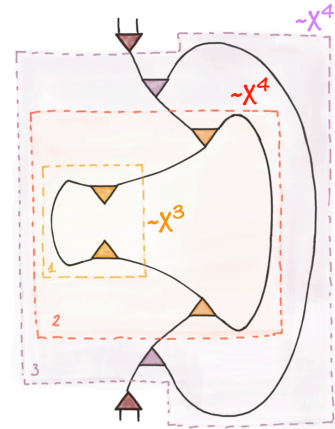


This is actually the way to bound the entanglement that a given subchain of length L can hold: we just need to count the number of virtual legs that need to be cut in order to split our subsystem from the rest. We can see that it will depend on the particular block of L sites: since by cutting one bond we split the system in two, there are blocks of length $\geq L$ that are connected to the TN by a single bond, and thus have entropy upper-bounded by a constant $\log \chi$, as in the MPS case (area law). However, for other blocks, the number of bonds that need to be cut may grow as $\log L$, and thus the entanglement of the block is upper-bounded by $\log \chi \log L$ (as in the critical case). This is illustrated in the figure, for the binary tree example (where, actually, the upper bound to the number of legs to be cut is $\log_2 L$).

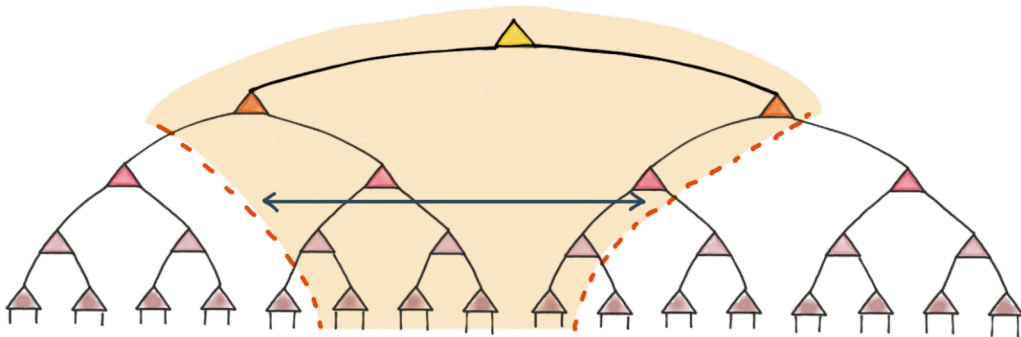


Trees can thus reproduce critical (power-law decaying) correlations in average (for instance, in an homogeneous system, one can construct a linear superposition of TTN translated with respect to each other).³⁸ They can also be used equally for PBC (same graph) and in higher dimensions.

The diagrams above also allow us to see that it is efficient to compute expectation values of local operators with this ansatz. For instance, the cost of computing the expectation values of a single-site operator is upper-bounded by the cost of computing the rdm for the two sites. this can be read from the diagram on the right, where the contraction costs of the different steps are indicated explicitly.

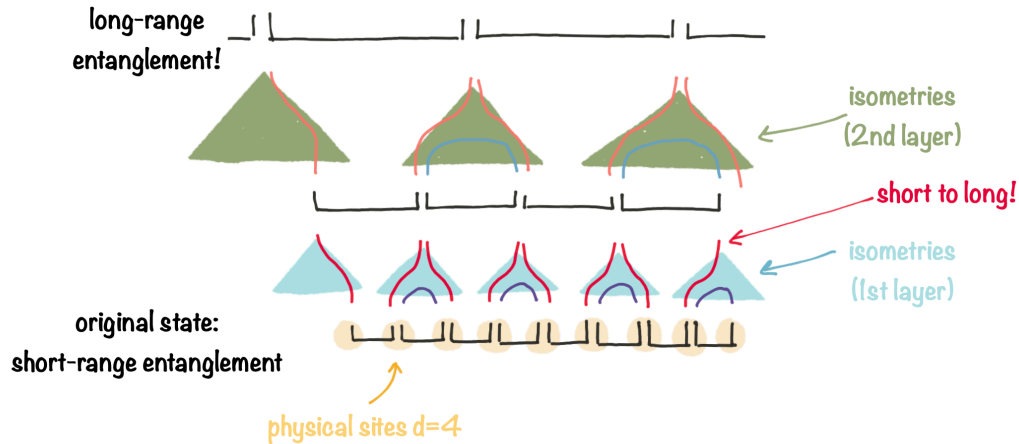


Notice that, even if we would consider a deeper tree, the cost of successive steps would not increase further than $O(\chi^4)$. This is due to the fact that the *causal cone*, i.e. the set of the TN “pinned” by a local operator (indicated in the following picture by a shadowed region), has a bounded width: the number of tensors included at each scale does not increase when moving up in the tree.



The property of being efficiently contractible is common for all TNS which do not contain loops (e.g. for MPS, but not for PEPS).

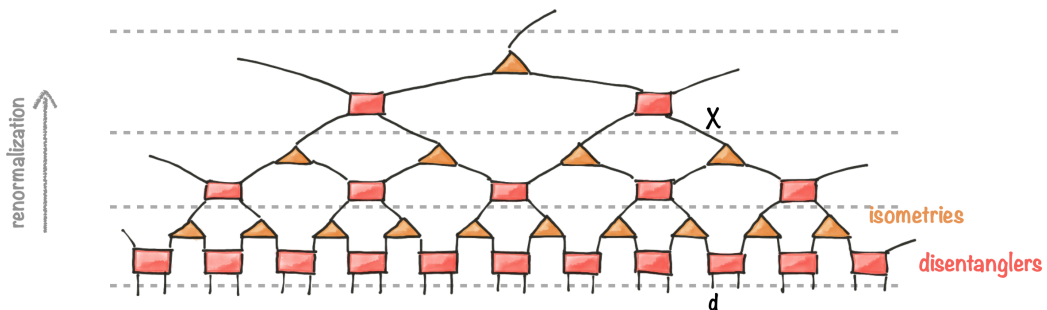
A drawback of TTN is that it cannot properly renormalize entanglement: short-range correlations can persist at arbitrarily large scales. Consider, for instance, a state with only short-range correlations, as illustrated in the lowest level of the next figure (notice the physical sites are composed of two qubits).



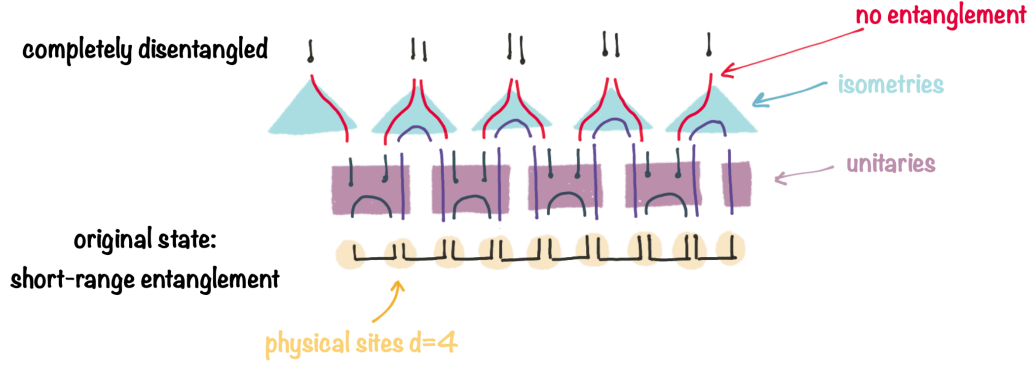
We can find a layer of isometries that reduces two sites to one (mapping $d^2 \rightarrow d$), but they cannot remove the entanglement *between* isometries, such that those correlations get now mapped to a longer length.

2. Multiscale entanglement renormalization ansatz (MERA)

To put remedy to the problem of TTN that we just described, G. Vidal introduced the MERA family.³⁹ Starting from the renormalization idea of TTN, in MERA an extra step is introduced, before each layer of isometries, to try to remove the inter-block entanglement. To do that, the ansatz introduces layers of unitary tensors, or *disentangler*s that can modify the entanglement between blocks of sites later blocked together by the isometries. The resulting TN then can be represented as the following figure (for a piece of a larger system).

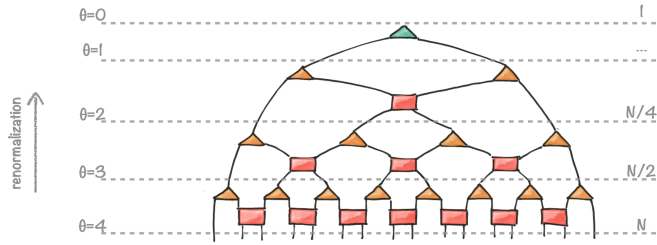


As a simple example, for the state with short-range correlations considered above, one layer of unitaries followed by one of isometries, as illustrated below, can completely remove the entanglement in the state. That means this state can be exactly represented by a MERA with only one renormalization step.



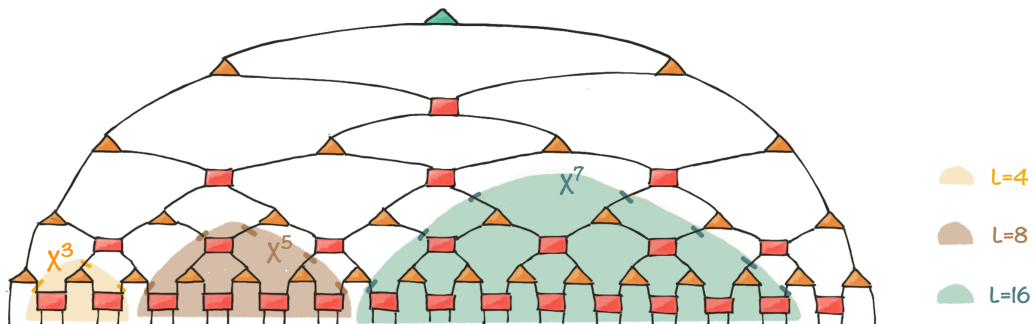
As in the case of the TTN, the MERA performs a renormalization of the physical degrees of freedom.

For a finite system of N sites, the number of layers (each layer consisting of a set of disentanglers and a set of isometries) is at most $\log_2 N$.



(Notice that other combinations are possible, e.g. 3-to-1 isometries). Counting the levels from the root of the MERA, at *level* θ , the number of effective sites is 2^θ . The total number of tensors can be easily computed to be $2N(1 - \frac{1}{N})$, i.e. it is upper-bounded by $2N$. Since the largest tensors are the disentanglers, with $O(\chi^4)$ components, the number of variational parameters in the MERA is thus $O(\chi^4 N)$.

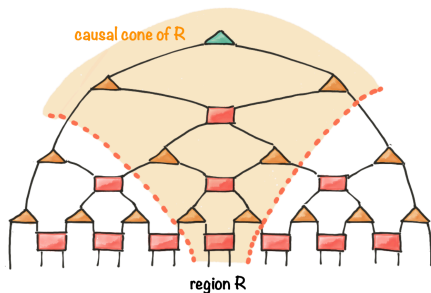
The entropy of a subchain can be upper-bounded by counting the number of legs that we need to cut to decouple the block from the TN. In contrast to the tree, we can see that in the MERA, all blocks can have entropy that scale as $\log L$ (they are not all equal, since the MERA structure breaks the translational symmetry, but the scaling is the same). In particular, in the figure we show several block sizes and the number of cuts corresponding to them, which in those cases is $2 \log_2 L - 1$.



The entropy of a subchain of length L is thus upper-bounded by $\sim \log \chi \log L$ and thus it violates the area law logarithmically, as in the case of critical chains.

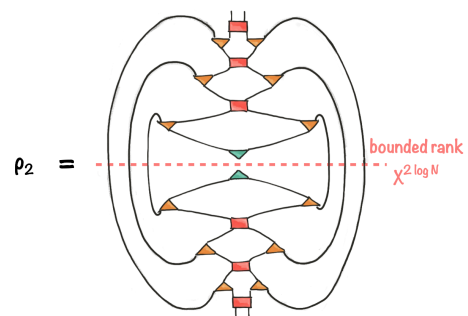
MERA can also be defined in higher dimensions. However, it has been proved that in two dimensions they can be efficiently mapped to PEPS,⁴⁰ and thus satisfy the area law. In particular, MERA are a subset of PEPS that can be efficiently contracted.

Although the TN in this case contains loops, certain expectation values can be contracted efficiently, which makes them suitable for numerical algorithms.⁴¹ This is thanks to the isometric and unitarity properties of the constituent tensors. It is the case of the norm (which reduces to the contraction of the root tensor with its adjoint), and of expectation values of local operators (i.e. acting on a region of constant size).



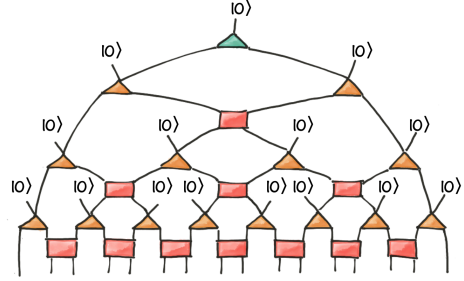
As in the case of TTN, the width of the causal cone for a region of fixed size is upper-bounded by a constant (it does not grow when moving up the renormalization steps).

Thus, it is possible to bound the computational cost of contracting these quantities. In particular, for the 2-site rdm, we obtain the figure on the right.



To see that the contraction can be done efficiently, we notice that the width is constant and the height is $\log_2 N$. If we contract layer by layer, starting from the innermost part of the diagram (root tensor), each step only requires contracting a fixed number of tensors, and thus the cost scales as $\text{poly}(\chi) \log N$. The same kind of scaling holds for higher dimensional MERA.

An interesting interpretation of MERA is as a quantum circuit⁴² that acts on a product state $|0\rangle^{\otimes N}$ and preparing the state: each isometry can be seen as a unitary that acts (downwards) on $|0\rangle$ and the state of a virtual bond.



Finally, one fundamental aspect of interest of MERA is their interpretation as implementing a renormalization group transformation: the tensors of the MERA can be used to map operators (for instance, the terms in the Hamiltonian) to higher scales, i.e. to a coarse-grained lattice.

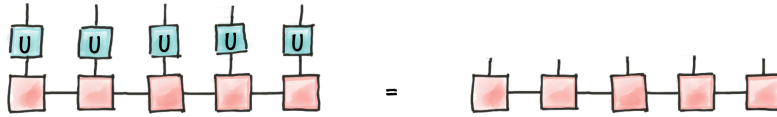
E. TNS and symmetries

Symmetric states can be built up from tensors with well-defined symmetries. In this way, the individual tensors are local building blocks that determine the physical properties of the collective state.

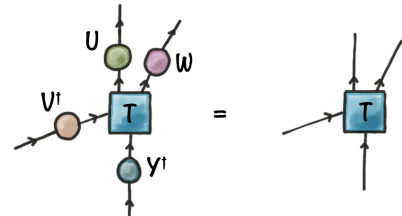
If a state has a *global* symmetry, it fulfills

$$U^{\otimes N}|\Psi\rangle = |\Psi\rangle,$$

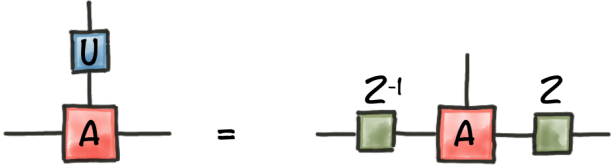
where U is a unitary transformation that acts on the physical indices. For a MPS, for instance,



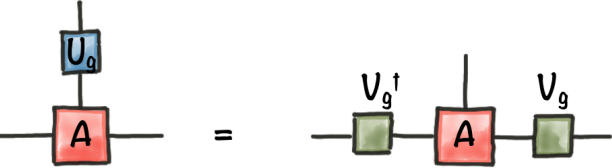
If all the individual tensors are symmetric, i.e. they remain invariant under acting with the transformation on all the legs, as illustrated, then the resulting state is invariant.



In the case of MPS and PEPS, because they satisfy a fundamental theorem that relates the tensors that represent the same state, the implication goes both ways: for an invariant state there is a representation with invariant tensors, namely the symmetry acts on the tensors as

$$\sum_j (U)_{ij} A^j = Z^{-1} A^i Z,$$


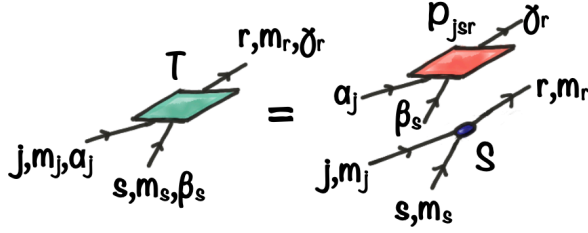
If the symmetry operation is a representation of a group G , i.e. $U_g^{\otimes N} |\Psi\rangle = |\Psi\rangle, \forall g \in G$, and $U_g U_h = U_{gh}$, the action of the transformation on the tensor is

$$\sum_j (U_g)_{ij} A^j = V_g^\dagger A^i V_g,$$


where V_g are representations of the group on the virtual spaces.

However, because there is a phase freedom (as a phase factor $V_g \rightarrow e^{i\phi_g} V_g$ would be compensated in V_g^\dagger), the V_g do not need to be linear representations but can be *projective representations*, satisfying $V_g V_h = e^{i\omega(g,h)} V_{gh}$. This is a very powerful result: the inequivalent projective representations actually classify the possible quantum phases under a symmetry in one dimension.^{43,44}

From the practical point of view, the invariance of the tensors implies that they can be decomposed,⁴⁵ and their structure can be exploited to have more efficient simulations, and explicitly invariant ansatzes. More concretely, the virtual space can be decomposed as a direct sum over the irreps of the group, and the virtual indices can be written as composite ones, $|\alpha\rangle = |j, m_j, \alpha_j\rangle$, where j indexes the irrep, m_j the states within it (e.g. for non-Abelian symmetries) and α_j are the *degeneracy* states, i.e. it runs over the dimension of the virtual space assigned to the j, m_j . Since virtual legs have assigned irrep labels, not all elements of the tensor are independent, but they are constrained by the symmetry. One of the simplest examples to visualize is that of a three legged-tensor (e.g. a MPS tensor), which, applying Wigner-Eckart theorem, can be decomposed in the product of a *degeneracy* tensor P , containing all variational parameters (the components not fixed by the symmetry) and one *structural* tensor, completely determined by the symmetry labels. Graphically:



$$T_{(jm_j \alpha_j), (sm_s \beta_s)}^{(rm_r \gamma_r)} = (P_{j sr})_{\alpha_j \beta_s}^{\gamma_r} S_{(jm_j)(sm_s)}^{(rm_r)}$$

For instance, in the $SU(2)$ case, for the example above the structural part will simply correspond to $S_{(jm_j)(sm_s)}^{(rm_r)} = \langle jm_j, sm_s | rm_r \rangle$, the Clebsch-Gordan coefficients. More general tensors can be either decomposed in interconnected three-legged pieces, or directly written as sums of blocks. A complete introduction to the practical treatment of symmetric tensors can be found in.⁴⁶

III. Representing operators as TN

A. Matrix product operators (MPO)

All the ansatzes discussed so far have been used only for pure states. They are actually descriptions of families of vectors in a vector space with a tensor product structure. As such, we can use the ansatzes more generally to describe operators. The most significant case is the one-dimensional matrix product operator (MPO).⁴⁷⁻⁴⁹

Operators acting on a many-body system can be expressed in a tensor product basis, such as $\{|i_k\rangle\langle j_k|\}_{i,j=0,\dots,d-1}^{\otimes N}$, or a Pauli basis $\{\sigma^\alpha\}^{\otimes N}$, with each $\{\sigma^\alpha\} := \{\frac{1}{2}, \frac{\sigma^x}{2}, \frac{\sigma^y}{2}, \frac{\sigma^z}{2}\}$. A MPO is simply an operator with coefficients in the chosen basis having MPS form. Explicitly,

$$O = \sum_{\{\alpha_k\}} \text{tr} \left(M_{[1]}^{\alpha_1} M_{[2]}^{\alpha_2} \dots M_{[N]}^{\alpha_N} \right) O_{[1]}^{\alpha_1} \otimes O_{[2]}^{\alpha_2} \otimes \dots \otimes O_{[N]}^{\alpha_N},$$

where the $O_{[k]}^{\alpha_k}$ are elements of a tensor product basis for the operator space.

1. MPO for local Hamiltonians

Many interesting operators can be written exactly (or approximately) in this form. Trivially, a tensor product operator is a MPO with bond dimension one. But also local operators

(for instance, local Hamiltonians) are MPOs with small bond dimension.

One of the simplest examples is the total magnetization of a spin 1/2 chain (a factor 1/2 is ignored for convenience),

$$S_x := \sum_k \sigma_{[k]}^x = \sigma_{[1]}^x \otimes \mathbb{1} \otimes \dots \otimes \mathbb{1} + \mathbb{1} \otimes \sigma_{[2]}^x \otimes \dots \otimes \mathbb{1} + \dots + \mathbb{1} \otimes \dots \otimes \mathbb{1} \otimes \sigma_{[N]}^x.$$

The last expression explicitly shows the coefficients of the operator in a product basis. we notice that these are exactly the same as those for the (unnormalized) W-state

$$|10\dots 0\rangle + |010\dots 0\rangle + \dots + |0\dots 01\rangle,$$

and thus the MPS tensors for that state are also valid for this operator, namely

$$M^0 = \begin{pmatrix} 1 & 0 \\ 0 & 1 \end{pmatrix}, \quad M^1 = \begin{pmatrix} 0 & 1 \\ 0 & 0 \end{pmatrix}.$$

The only difference is that they will be coefficients in a different basis, in which we identify $|0\rangle \equiv \mathbb{1}$ and $|1\rangle \equiv \sigma^x$.

For MPOs it is common to use another way of writing the 4-legged tensors, which have elements $\tilde{M}_{\ell r}^{ij} = \sum_{\alpha} M_{\ell r}^{\alpha} O_{ij}^{\alpha}$, by showing them as operator valued matrices, where the indices of the matrices correspond to the virtual degrees of freedom (as in the example shown above) and the physical indices are written in a compact way as an operator. More concretely, the operator in element (ℓr) is $\tilde{M}_{\ell r} = \sum_{\alpha} M_{\ell r}^{\alpha} O^{\alpha}$.

For instance, for the previous case,

$$\tilde{M} = \begin{pmatrix} \mathbb{1} & \sigma^x \\ 0 & \mathbb{1} \end{pmatrix}.$$

Notice that the tensors for the edge sites will be different (the same as for the OBC MPS), with

$$\tilde{M}_{[1]} = \begin{pmatrix} \mathbb{1} & \sigma^x \end{pmatrix}, \quad \tilde{M}_{[N]} = \begin{pmatrix} \sigma^x \\ \mathbb{1} \end{pmatrix}.$$

The middle tensors in this particular example are all equal, but we can change the weights of the different terms to represent a position-dependent operator $\sum_k C_k \hat{O}_{[k]}$ for any single site operator $\hat{O}_{[k]}$ with essentially the same construction, only allowing the \tilde{M} tensors to depend on the site k by changing $\sigma^x \rightarrow C_k \hat{O}_{[k]}$.

Any sum of nearest-neighbour operators (in particular, nearest-neighbour Hamiltonians) can be constructed in a similar way. But also other operators that are sums of terms with a regular structure.

2. Finite state automata and MPS/MPO

A more general perspective is provided by the connection between MPS/MPO and *finite state automata* (FSA).

In computer science, FSA are a computation model that accepts regular expressions. A FSA is defined by

- a set of states S , containing an initial state s_0 and a (set of) final state;
- an input alphabet Σ , i.e. a set of symbols which can be accepted;
- a *transition function*, i.e. a set of possible transitions between states triggered by the input $S \times \Sigma \rightarrow S$.

If the automaton is in a certain state s , it can accept a symbol $\varepsilon \in \Sigma$ and at the same time change its state to $s' \in S$ if it contains a transition $(s, \varepsilon) \rightarrow s'$. Starting in the initial state, the FSA *accepts* a certain string if it sequentially accepts all its symbols and ends up in a final state.

MPS (or MPO) with open boundary conditions can also be seen as FSA with a fixed number of transitions⁵⁰ in the following way:

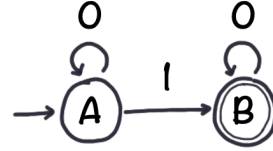
- each distinct value of the virtual bond corresponds to a state of the FSA,
- the different values of the physical index (which label the states of the local bases) correspond to the input symbols,
- each non-vanishing element of the MPS tensor $A_{\ell r}^i \neq 0$ corresponds to a valid transition of the automaton $(\ell, i) \rightarrow r$, which graphically we represent as

$$\begin{array}{c} i \\ | \\ \square \\ | \\ \ell \quad r \end{array} = x$$

As a simple example we may consider the W-state (equivalently, the local operator $S_x = \sum_k \sigma_{[k]}^x$) discussed above. The regular expression that includes all components of the state is

0^*10^* (matches any string that contains exactly one character 1, and any number of 0s). The following FSA, represented on the right by its state diagram (in which an arrow indicates the initial state and a double line the final one), recognizes this pattern:

- $S = \{A, B\}$, $s_0 = A$, $F = \{B\}$,
- $\Sigma = \{0, 1\}$,
- $\delta = \{(A, 0) \rightarrow A, (A, 1) \rightarrow B, (B, 0) \rightarrow B\}$.



In the MPS representation, the same transition function corresponds to

$$\begin{array}{c} 0 \\ | \\ \square \\ | \\ A \end{array} - \begin{array}{c} \square \\ | \\ A \end{array} = 1, \quad \begin{array}{c} 1 \\ | \\ \square \\ | \\ A \end{array} - \begin{array}{c} \square \\ | \\ B \end{array} = 1, \quad \begin{array}{c} 0 \\ | \\ \square \\ | \\ B \end{array} - \begin{array}{c} \square \\ | \\ B \end{array} = 1$$

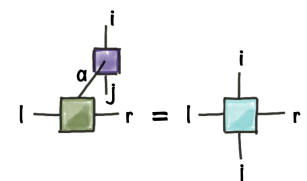
where we interpret A and B as two different labels for the virtual bonds, which means the required bond dimension is $D = 2$. So that the MPS describes a chain of length N , we need to fix the length of the input strings (i.e. the number of tensors) to N , and demand that the boundary tensors ensure the desired initial and final states. The left virtual index of the first tensor must thus in this case correspond to the index A , while the right virtual index of the last tensor needs to be B . Equivalently, the edge bonds of the tensors at the boundary have dimension 1, and we can specify only their non-vanishing components, namely

$$\begin{array}{c} 0 \\ | \\ \square \\ | \\ A \end{array} = 1, \quad \begin{array}{c} 1 \\ | \\ \square \\ | \\ B \end{array} = 1$$

$$\begin{array}{c} 1 \\ | \\ \square \\ | \\ A \end{array} = 1, \quad \begin{array}{c} 0 \\ | \\ \square \\ | \\ B \end{array} = 1$$

It is easy to check that these elements correspond precisely to the M tensors explicitly written above. The input symbols 0 and 1 correspond to the states of the physical local basis in the case of the W-state.

If we are trying to write the MPO for a magnetization $S_\beta = \sum_k \sigma_{[k]}^\beta$, we can identify the symbols with operators $0 \equiv \mathbb{1}$, $1 \equiv \sigma^\beta$. This conversion from the input label to the operator elements in the physical basis can also be represented (and computed) as a tensor contraction, as indicated in the figure.



Notice that the non-vanishing elements of the tensor can be of different magnitude (and they can be complex), which allows us to represent sums of terms with regular structure but having different coefficients.

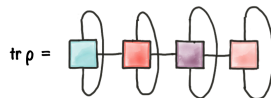
In a similar way one can find the MPO for any nearest neighbour Hamiltonian (e.g. the Ising term requires $D = 2$ because there is one extra *state* needed, corresponding to the intermediate position in the two-body term). If the range of the terms increases, so does in general the bond dimension required in the MPO, although there are exceptions that can be written exactly with small bond dimension. For instance, exponentially decaying interactions can be written with small bond dimension, while algebraically decaying ones need a bond dimension that grows with the system size. Nevertheless, they can be approximated as a sum of exponentials.⁴⁹

The FSA construction is mostly useful to exactly write certain operators as MPO. In other scenarios, MPOs are used to approximate operators, for instance in order to apply time evolution to a certain state. In that case, a Suzuki-Trotter expansion (but also other approximation schemes) can be applied to write the evolution operator in terms of pieces which can themselves be expressed as MPOs.

3. MPO as ansatz for density operators

The MPO can also be used as a variational ansatz, to represent mixed states, for instance, systems in thermal equilibrium or open systems in interaction with a bath. But while a (not identically null) MPS always defines a physically valid state (the only condition being it to be normalized), not all operators are valid density matrices. MPO representing density operators (MPDOs) have to satisfy the following physical conditions.

- Normalization, $\text{tr} \rho = 1$. Computing the trace of a MPO can be done efficiently, as indicated by the diagram. Thus, it is possible to normalize the MPO dividing by the result of this contraction (if the latter does not vanish).



- Hermiticity, $\rho = \rho^\dagger$. Given a MPO that is not Hermitian, we can always take its Hermitian part, by summing the MPO with its Hermitian conjugate (which is also a

MPO with the same bond dimension).

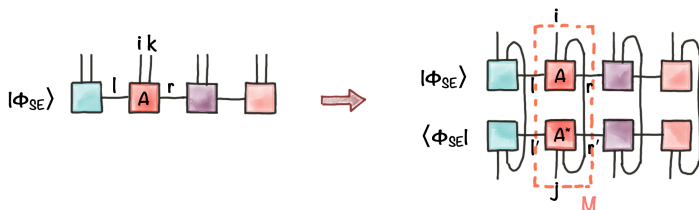
$$\begin{array}{c} \text{---} \\ | \\ \text{---} \end{array} \begin{array}{c} \text{---} \\ | \\ \text{---} \end{array} \begin{array}{c} \text{---} \\ | \\ \text{---} \end{array} \begin{array}{c} \text{---} \\ | \\ \text{---} \end{array} + \left(\begin{array}{c} \text{---} \\ | \\ \text{---} \end{array} \right)^*$$

This will also produce a MPO (with, in general, doubled bond dimension), and thus can be imposed within the MPO framework.

- Positivity, $\rho \geq 0$, is a different story: the condition for a matrix to be positive semidefinite is not a local one, in a many-body operator, but involves all the spectrum of the matrix, which is exponentially costly to compute and thus virtually impossible for sufficiently large systems.

Recall that a Hermitian matrix is said to be positive semidefinite, denoted $M \geq 0$ if all its eigenvalues are non-negative. In the MPO case, in fact, if we are given the tensors, it is a very hard problem to decide whether the MPO is or not positive: for a finite system, it is NP-hard, and it is undecidable in the thermodynamic limit.⁵¹

The first two conditions can be imposed within the form of a MPO, but positivity cannot. However, one can define a more restrictive family of MPOs that are positive by construction: the *purification ansatz*.^{47,52} We know that for any mixed state there exists a purification, i.e. a pure state defined on an enlarged system with an additional environment, such that tracing out the ancilla returns the mixed state of the system. The purification ansatz (MPDO) corresponds to assuming for the purification a particular structure, where for each system site, we introduce an ancillary site of the same dimension, and group them together in an effective site of squared physical dimension.

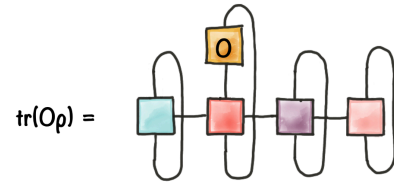


The purified state $|\Phi\rangle_{SE}$ is assumed to have a MPS structure in this basis, and to be normalized, and the MPDO is obtained when tracing out the ancillary sites, as shown in the picture.

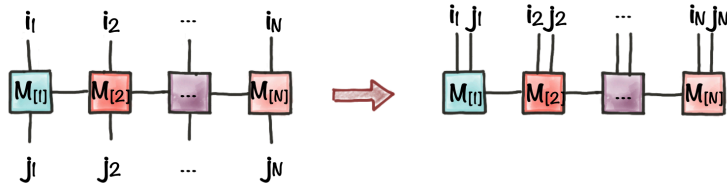
Because it is constructed from the partial trace of a normalized state, the resulting MPDO is a valid physical state. But it is not the most general MPO, because the tensors have a particular structure, $M_{\tilde{\ell}\tilde{r}} = \sum_k A_{\ell_r}^{ik} A_{\ell'_r}^{jk}$, with $\tilde{\ell} = (\ell, \ell')$ (same for \tilde{r}). In practice, it is possible to use this positive ansatz in numerics (although the algorithms become less efficient, because higher degree dependence on the variational parameters A mean that iterative numerical methods have to be used).

Given a MPO which is positive, it may be that expressing it exactly as a purification requires exponentially large bond dimension.⁵² However, it is possible to find an efficient approximation with the purification form.

Computing expectation values in a MPO involves calculating traces like $\text{tr}(O\rho)$, illustrated in the figure, which can be done efficiently.



Notice that a MPO can be mapped to a MPS by *vectorizing* it, i.e. by mapping the basis elements to vectors as $|i\rangle\langle j| \rightarrow |i\rangle|j\rangle$. Graphically,



This allows us to use MPS algorithms and routines on MPOs. In particular, the expectation value shown above can be written as the contraction of two vectors, each one corresponding to a vectorized MPO, $\text{tr}(O\rho) = \langle O^\dagger | \rho \rangle$. Notice that the scalar product on the right is equivalent to the Hilbert-Schmidt product of operators $\langle A|B \rangle = \text{tr}(A^\dagger B)$. Alternatively, we can also write the same quantity as a contraction of a MPO between two MPS, the latter corresponding to vectorized operators for ρ and the identity, and the MPO being a *superoperator* that acts as O on the first (output) indices of $|\rho\rangle$ and as identity on the others, i.e. $\text{tr}(O\rho) = \langle \mathbb{1} | O \otimes \mathbb{1} | \rho \rangle$. Notice that in this case, the vectorized $|Id\rangle$ is not a normalized MPS. In diagrams,

$$\text{tr}(O\rho) = \langle \mathbb{1} | \text{---} \text{---} \text{---} \text{---} |\rho\rangle = \langle \mathbb{1} | O \otimes \mathbb{1} |\rho\rangle$$

If we consider the purification ansatz, $\rho = \text{tr}_E(|\Phi_{SE}\rangle\langle\Phi_{SE}|)$, the expectation values reduce to a simple expectation value in the purified state, $\text{tr}(O\rho) = \text{tr}_S(O\text{tr}_E(|\Phi_{SE}\rangle\langle\Phi_{SE}|)) = \langle\Phi_{SE}|O_S \otimes \mathbb{1}_E|\Phi_{SE}\rangle$, with the operator acting only non-trivially on the system indices, and as the identity on the environment ones. Graphically,

$$\langle \mathbb{1} | O \otimes \mathbb{1} |\Phi_{SE}\rangle = \langle \Phi_{SE} | \text{---} \text{---} \text{---} \text{---} |\Phi_{SE}\rangle$$

4. Thermal states

The purification ansatz is very natural for thermal states. The thermal equilibrium state of a system with Hamiltonian H at inverse temperature β is given by the Gibbs ensemble,

$$\rho_\beta = \frac{e^{-\beta H}}{\text{tr}(e^{-\beta H})}$$

A purification of this state is the so-called *thermofield double state*,

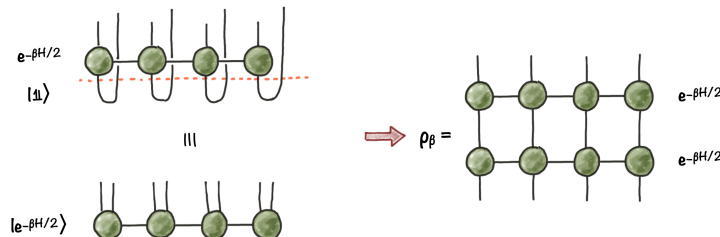
$$|\Psi_\beta\rangle = \frac{1}{\sqrt{Z}} \sum_n e^{-\beta E_n/2} |E_n\rangle_S |E_n\rangle_A,$$

where $Z = \text{tr}(e^{-\beta H})$ is the partition function, and the sum runs over all eigenstates of the Hamiltonian, $H|E_n\rangle = E_n|E_n\rangle$. The subindices S (A) indicate the original system and a copy, the ancilla. We can rewrite the state as

$$|\Psi_\beta\rangle = \frac{1}{\sqrt{Z}} e^{-\beta H/2} \sum_n |E_n\rangle_S |E_n\rangle_A \propto (e^{-\beta H/2} \otimes \mathbb{1}) |\mathbb{1}\rangle_{SA},$$

where the vector $|\mathbb{1}\rangle_{SA}$ is (up to normalization) a maximally entangled state between system and ancilla. As written above, the exponential operator acts on the first set of indices (S), but it can also be chosen to act on the ancilla only, or split as $e^{-\beta H/4} \otimes e^{-\beta H^T/4}$ (where the transposition results from the vectorizing map).

We know that MPO are good to approximate Gibbs states of local Hamiltonians, i.e. operators of the form $e^{-\beta H}$ can be efficiently approximated by this ansatz. By constructing such approximation for $\beta/2$ and vectorizing it, which is equivalent to acting with it on the vectorized identity, we have a purification for the thermal state. Graphically,



Usually, the MPO approximation of $e^{-\beta H/2}$ is found in practice by applying imaginary time evolution to the identity via a Suzuki-Trotter expansion. This can then be used to compute expectation values in thermal equilibrium, but also to simulate evolution in real time and compute thermal response functions.⁵³

B. PEPOs

Like the MPS, the MPO construction can also be naturally generalized to higher dimensional lattices. In that case, we can define a PEPO (projected entangled pair operator). This ansatz can be used also to approximate density operators and, in particular thermal states (either directly or, more commonly, through a purification). Of course, it is also possible to describe exactly local interactions, even though this is much less used in practical calculations than the analogous MPO, due to the computational costs of the algorithms.

¹ S. R. White, Phys. Rev. Lett. **69**, 2863 (1992).

² U. Schollwöck, Annals of Physics **326**, 96 (2011), 1008.3477.

- ³ B.-X. Zheng, C.-M. Chung, P. Corboz, G. Ehlers, M.-P. Qin, R. M. Noack, H. Shi, S. R. White, S. Zhang, and G. K.-L. Chan, *Science* **358**, 1155 (2017), <https://science.sciencemag.org/content/358/6367/1155.full.pdf>.
- ⁴ G. K.-L. Chan and S. Sharma, *Annual Review of Physical Chemistry* **62**, 465 (2011), pMID: 21219144, <https://doi.org/10.1146/annurev-physchem-032210-103338>.
- ⁵ T. Nishino, *Journal of the Physical Society of Japan* **64**, 3598 (1995), <https://doi.org/10.1143/JPSJ.64.3598>.
- ⁶ M. Levin and C. P. Nave, *Phys. Rev. Lett.* **99**, 120601 (2007).
- ⁷ J. I. Cirac and F. Verstraete, *Journal of Physics A: Mathematical and Theoretical* **42**, 504004 (2009).
- ⁸ F. Verstraete, V. Murg, and J. Cirac, *Advances in Physics* **57**, 143 (2008), 0907.2796.
- ⁹ R. Orús, *Annals Phys.* **349**, 117 (2014), arXiv:1306.2164 [cond-mat.str-el].
- ¹⁰ J. C. Bridgeman and C. T. Chubb, *Journal of Physics A: Mathematical and Theoretical* **50**, 223001 (2017).
- ¹¹ P. Silvi, F. Tschirsich, M. Gerster, J. Jünemann, D. Jaschke, M. Rizzi, and S. Montangero, *SciPost Phys. Lect. Notes* **8** (2019).
- ¹² M. A. Nielsen and I. L. Chuang, *Quantum Computation and Quantum Information: 10th Anniversary Edition*, 10th ed. (Cambridge University Press, New York, NY, USA, 2011).
- ¹³ J. Eisert, M. Cramer, and M. B. Plenio, *Rev. Mod. Phys.* **82**, 277 (2010).
- ¹⁴ M. B. Hastings, *J. Stat. Mech.* **2007**, P08024 (2007).
- ¹⁵ R. Movassagh and P. W. Shor, *Proceedings of the National Academy of Sciences* **113**, 13278 (2016), <https://www.pnas.org/content/113/47/13278.full.pdf>.
- ¹⁶ M. M. Wolf, F. Verstraete, M. B. Hastings, and J. I. Cirac, *Phys. Rev. Lett.* **100**, 070502 (2008).
- ¹⁷ I. Affleck, T. Kennedy, E. H. Lieb, and H. Tasaki, *Phys. Rev. Lett.* **59**, 799 (1987).
- ¹⁸ D. Perez-García, F. Verstraete, M. M. Wolf, and J. I. Cirac, *Quantum Inf. Comput.* **7**, 401 (2007), quant-ph/0608197.
- ¹⁹ C. Schön, E. Solano, F. Verstraete, J. I. Cirac, and M. M. Wolf, *Phys. Rev. Lett.* **95**, 110503 (2005).
- ²⁰ B. Pirvu, G. Vidal, F. Verstraete, and L. Tagliacozzo, *Phys. Rev. B* **86**, 075117 (2012).
- ²¹ F. Verstraete and J. I. Cirac, *Phys. Rev. B* **73**, 094423 (2006).

- ²² E. H. Lieb and D. W. Robinson, *Communications in Mathematical Physics* **28**, 251 (1972).
- ²³ N. Schuch, I. Cirac, and D. Pérez-García, *Annals of Physics* **325**, 2153 (2010).
- ²⁴ A. Kitaev, *Annals of Physics* **303**, 2 (2003).
- ²⁵ P. Corboz, P. Czarnik, G. Kapteijns, and L. Tagliacozzo, *Phys. Rev. X* **8**, 031031 (2018).
- ²⁶ M. Rader and A. M. Läuchli, *Phys. Rev. X* **8**, 031030 (2018).
- ²⁷ N. Schuch, M. M. Wolf, F. Verstraete, and J. I. Cirac, *Phys. Rev. Lett.* **98**, 140506 (2007).
- ²⁸ M. C. Bañuls, D. Pérez-García, M. M. Wolf, F. Verstraete, and J. I. Cirac, *Phys. Rev. A* **77**, 052306 (2008).
- ²⁹ D. Perez-García, F. Verstraete, J. I. Cirac, and M. M. Wolf, *Quantum Information and Computation* **8**, arXiv:0707.2260 (2008), arXiv:0707.2260 [quant-ph].
- ³⁰ M. B. Hastings, *Phys. Rev. B* **73**, 085115 (2006).
- ³¹ A. Molnar, N. Schuch, F. Verstraete, and J. I. Cirac, *Phys. Rev. B* **91**, 045138 (2015).
- ³² J. I. Cirac, D. Poilblanc, N. Schuch, and F. Verstraete, *Phys. Rev. B* **83**, 245134 (2011).
- ³³ N. Schuch, D. Poilblanc, J. I. Cirac, and D. Pérez-García, *Phys. Rev. Lett.* **111**, 090501 (2013).
- ³⁴ J. I. Cirac, J. Garre-Rubio, and D. Pérez-García, *Revista Matemática Complutense* **32**, 579 (2019).
- ³⁵ G. Scarpa, A. Molnár, Y. Ge, J. J. García-Ripoll, N. Schuch, D. Pérez-García, and S. Iblisdir, *Phys. Rev. Lett.* **125**, 210504 (2020).
- ³⁶ I. Cirac, D. Perez-Garcia, N. Schuch, and F. Verstraete, “Matrix product states and projected entangled pair states: Concepts, symmetries, and theorems,” (2020), arXiv:2011.12127 [quant-ph].
- ³⁷ Y.-Y. Shi, L.-M. Duan, and G. Vidal, *Phys. Rev. A* **74**, 022320 (2006).
- ³⁸ P. Silvi, V. Giovannetti, S. Montangero, M. Rizzi, J. I. Cirac, and R. Fazio, *Phys. Rev. A* **81**, 062335 (2010).
- ³⁹ G. Vidal, *Phys. Rev. Lett.* **99**, 220405 (2007).
- ⁴⁰ T. Barthel, M. Kliesch, and J. Eisert, *Phys. Rev. Lett.* **105**, 010502 (2010).
- ⁴¹ G. Evenbly and G. Vidal, *Phys. Rev. B* **79**, 144108 (2009).
- ⁴² G. Vidal, *Phys. Rev. Lett.* **101**, 110501 (2008).
- ⁴³ X. Chen, Z.-C. Gu, and X.-G. Wen, *Phys. Rev. B* **83**, 035107 (2011).
- ⁴⁴ N. Schuch, D. Pérez-García, and I. Cirac, *Phys. Rev. B* **84**, 165139 (2011).
- ⁴⁵ S. Singh, R. N. C. Pfeifer, and G. Vidal, *Phys. Rev. A* **82**, 050301 (2010).

- ⁴⁶ C. Hubig, “Symmetry-protected tensor networks,” (2017).
- ⁴⁷ F. Verstraete, J. J. García-Ripoll, and J. I. Cirac, Phys. Rev. Lett. **93**, 207204 (2004), cond-mat/0406426.
- ⁴⁸ M. Zwolak and G. Vidal, Phys. Rev. Lett. **93**, 207205 (2004).
- ⁴⁹ B. Pirvu, V. Murg, J. I. Cirac, and F. Verstraete, New Journal of Physics **12**, 025012 (2010), 0804.3976.
- ⁵⁰ G. M. Crosswhite and D. Bacon, Phys. Rev. A **78**, 012356 (2008).
- ⁵¹ M. Kliesch, D. Gross, and J. Eisert, Phys. Rev. Lett. **113**, 160503 (2014).
- ⁵² G. D. las Cuevas, N. Schuch, D. Pérez-García, and J. I. Cirac, New Journal of Physics **15**, 123021 (2013).
- ⁵³ T. Barthel, New Journal of Physics **15**, 073010 (2013).